

This is the author-created version of the following work:

McCoy-West, A.J., Mortimer, N., Burton, K.W., Ireland, T.R., and Cawood, P.A.
(2021) *Re-initiation of plutonism at the Gondwana margin after a magmatic*
hiatus: the bimodal Permian-Triassic Longwood Suite, New Zealand. Gondwana
Research, . (In Press)

Access to this file is available from:

<https://researchonline.jcu.edu.au/69723/>

Published Version: © 2021 Published by Elsevier B.V. on behalf of International Association for Gondwana Research. Accepted Version: © 2021. This manuscript version is made available under the CC-BY-NC-ND 4.0 license

<http://creativecommons.org/licenses/by-nc-nd/4.0/>

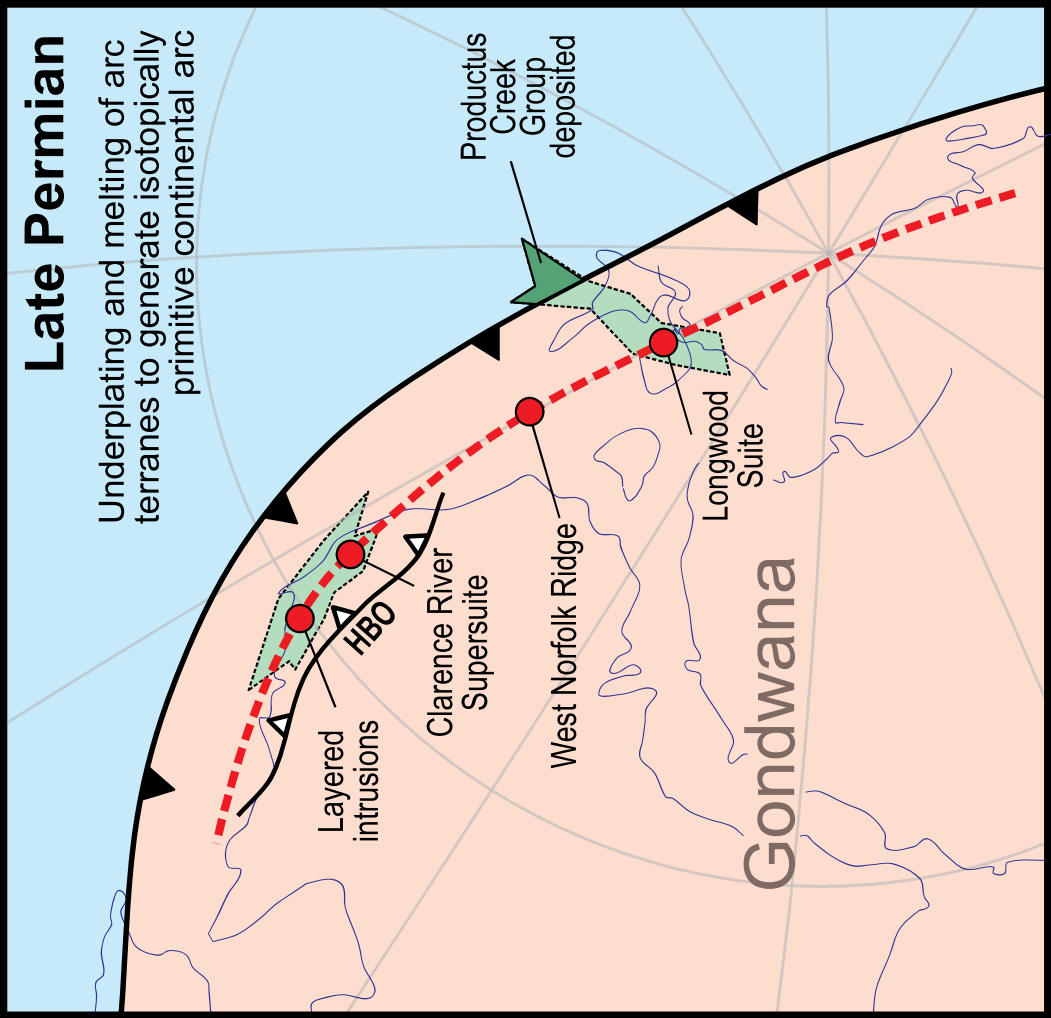
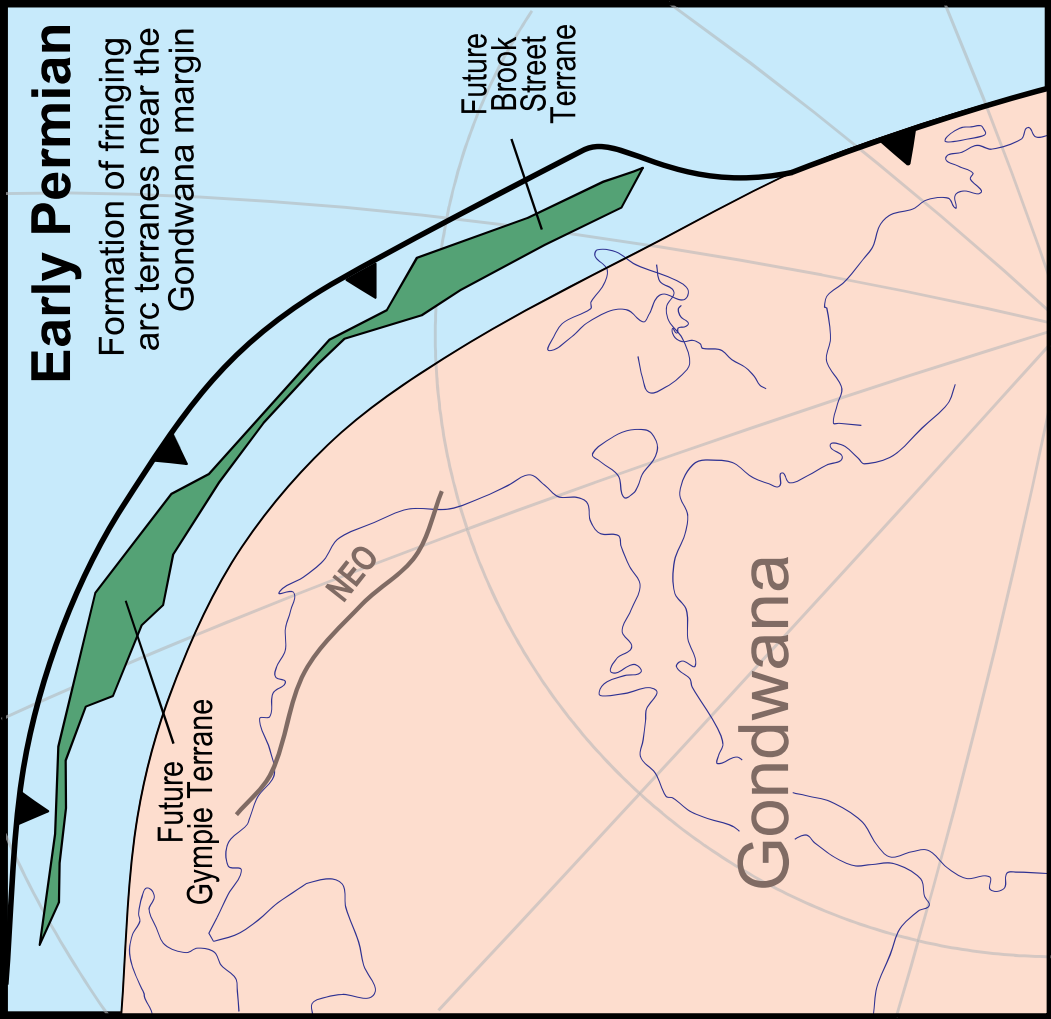
Please refer to the original source for the final version of this work:

<https://doi.org/10.1016/j.gr.2021.09.021>

Gondwana Research

Re-initiation of plutonism at the Gondwana margin after a magmatic hiatus: The bimodal Permian-Triassic Longwood Suite, New Zealand --Manuscript Draft--

Manuscript Number:	GWR-D-21-00190R4
Article Type:	Research Paper
Keywords:	Trondhjemite; U-Pb geochronology, radiogenic Sr-Nd, stable Nd; Darran Suite; Brook Street Terrane; Separation Point Suite.
Corresponding Author:	Alex J McCoy-West, Ph.D. James Cook University Townsville, QLD AUSTRALIA
First Author:	Alex J McCoy-West, Ph.D.
Order of Authors:	Alex J McCoy-West, Ph.D. Nick Mortimer Kevin Burton Trevor Ireland Peter Cawood
Abstract:	<p>The Cambrian to Cretaceous Tuhua Intrusives, New Zealand, preserve an igneous record of Phanerozoic subduction and crustal growth at the margin of Gondwana. Within the Tuhua Intrusives, the coeval gabbroic and trondhjemitic intrusions of the c. 261-243 Ma Longwood Suite stand out as being isotopically more primitive and chemically distinct from all other New Zealand plutonic suites. We present new U-Pb crystallization ages, trace element analyses and Sr-Nd isotope compositions of the Longwood Suite. U-Pb SHRIMP zircon ages of 258.5 ± 2.5 Ma, 256.0 ± 1.8 Ma, 247.8 ± 2.7 Ma and 243.2 ± 2.4 Ma obtained from plutons on Ruapuke Island, and a dike at Bluff, affirm the restricted time range and expand the known areal extent of the Longwood Suite. Longwood Suite granitoids are I-type and sodic ($K/Na < 0.4$), with distinctive low Rb and Nb/Ta, flat rare earth element patterns ($La/Yb \text{ N} < 10$), unradiogenic $^{87}Sr/^{86}Sr(t)$ (0.7029 to 0.7032) and radiogenic $\epsilon^{143}Nd(t)$ (+6.3 to +8.2), compared to the nearby, calc-alkaline, Late Triassic Darran Suite I-type plutons of the Tuhua Intrusives. Stable Nd isotope ratios of Longwood Suite samples are highly variable (-0.075 ‰ to $+0.158 \text{ ‰}$; $\delta^{146}/^{144}Nd = 233 \text{ ppm}$) compared to global plutonic rocks ($\delta^{146}/^{144}Nd = 44 \text{ ppm}$). Collectively, the above geochemical characteristics are consistent with generation of the granitoids by shallow (garnet-absent) melting of an amphibolitic residue, from which we infer relatively thin lithosphere. The Longwood Suite has a maximum areal addition rate of $43 \text{ km}^2/\text{Ma}$, substantially less than the subsequent plutonic suites when the magmatic arc was fully established. We suggest a petrotectonic model whereby thinned Gondwana continental margin crust was tectonically underplated by Permian intra-oceanic island arc crust and mantle lithosphere, which subsequently melted to generate the isotopically primitive bimodal trondhjemite and gabbro plutons of the Longwood Suite.</p>
Response to Reviewers:	...



Research Highlights

- The primitive bimodal magmatism of the Longwood Suite occurred from 261-243 Ma
- Granitoid geochemistry requires shallow melting of an amphibolitic residue
- The Longwood Suite has a significantly lower areal addition rate than the later arc
- Thinned Gondwana crust was tectonically underplated by Permian arc lithosphere

Re-initiation of plutonism at the Gondwana margin after a magmatic hiatus: The bimodal Permian-Triassic Longwood Suite, New Zealand

AJ McCoy-West^{1,2*}, N Mortimer³, KW Burton⁴, TR Ireland⁵ and PA Cawood²

¹*Earth and Environmental Sciences, James Cook University, Townsville, QLD 4811, Australia*

²*Department of Earth, Atmosphere and Environment, Monash University, Clayton, Victoria, 3800, Australia*

³*GNS Science, Dunedin Research Centre, Dunedin, 9054, New Zealand*

⁴*Department of Earth Sciences, Durham University, Science Laboratories, Durham, DH1 3LE, UK*

⁵*Research School of Earth Sciences, Australian National University, Canberra, 0200, Australia*

Number of words: 7417

Number of references: 129

Number of figures: 11

Number of tables: 3

Corresponding author: Alex McCoy-West (alex.mccoywest@jcu.edu.au)

Keywords: Trondhjemite; U-Pb geochronology; radiogenic Sr-Nd; stable Nd; Longwood Suite; Darran Suite; Brook Street Terrane; Separation Point Suite.

Abstract

The Cambrian to Cretaceous Tuhua Intrusives, New Zealand, preserve an igneous record of Phanerozoic subduction and crustal growth at the margin of Gondwana. Within the Tuhua Intrusives, the coeval gabbroic and trondhjemitic intrusions of the c. 261-243 Ma Longwood Suite stand out as being isotopically more primitive and chemically distinct from all other New Zealand plutonic suites. We present new U-Pb crystallization ages, trace element analyses and Sr-Nd isotope compositions of the Longwood Suite. U-Pb SHRIMP zircon ages of 258.5 ± 2.5 Ma, 256.0 ± 1.8 Ma, 247.8 ± 2.7 Ma and 243.2 ± 2.4 Ma obtained from plutons on Ruapuke Island, and a dike at Bluff, affirm the restricted time range and expand the known areal extent of the Longwood Suite. Longwood Suite granitoids are I-type and sodic ($K/Na < 0.4$), with distinctive low Rb and Nb/Ta, flat rare earth element patterns ($La/Yb_N < 10$), unradiogenic $^{87}Sr/^{86}Sr_{(t)}$ (0.7029 to 0.7032) and radiogenic $\epsilon^{143}Nd_{(t)}$ (+6.3 to +8.2), compared to the nearby, calc-alkaline, Late Triassic Darran Suite I-type plutons of the Tuhua Intrusives. Stable Nd isotope ratios of Longwood Suite samples are highly variable ($\delta^{146/144}Nd = 233$ ppm) compared to global plutonic rocks ($\delta^{146/144}Nd = 44$ ppm) and reflect the removal of phosphate minerals. Collectively, these geochemical characteristics are consistent with generation of the granitoids by shallow (garnet-absent) melting of an amphibolitic residue, from which we infer relatively thin lithosphere. The Longwood Suite has a maximum areal addition rate of $43 \text{ km}^2/\text{Ma}$, substantially less than the subsequent plutonic suites when the magmatic arc was fully established. We suggest a petrotectonic model whereby Gondwana continental margin crust was tectonically underplated by Permian intra-oceanic island arc crust and mantle lithosphere, which subsequently melted to generate the isotopically primitive gabbro and trondhjemitic plutons of the Longwood Suite.

1.0 Introduction

Zealandia is Earth's most recently recognized continent (Mortimer and Campbell, 2014; Mortimer et al., 2017), with the oldest known rocks being the Middle Cambrian limestones of the Takaka Terrane and c. 500 Ma plutons of the Jaquiery Suite (Mortimer et al., 2014). No exposed Precambrian crust has been discovered to date, although isotopic evidence suggests more ancient lower crustal and sub-continental lithospheric mantle domains exist at depth (e.g. Liu et al., 2015; McCoy-West et al., 2016; McCoy-West et al., 2013; Turnbull et al., 2021). Despite these hints of ancient lithospheric roots, Zealandia's crustal history is reflective of Cambrian to Early Cretaceous growth and accretion of terranes and batholiths at the southeastern margin of Gondwana, followed by Late Cretaceous continental rifting and breakup, and Cenozoic drift and dispersal as a separate post-Gondwana continent. As such it provides an ideal setting to investigate a range of inter-related crustal growth and stabilisation processes. The Median Batholith (Mortimer et al., 1999b) that bisects Zealandia and represents a long-lived (c. 495-105 Ma), regional arc-root plutonic complex (10,200 km²) preserves the intrusive record of subduction related magmatism at the Gondwana margin throughout much of the Phanerozoic (e.g. Muir et al., 1996b; Schwartz et al., 2017; Tulloch and Kimbrough, 2003), with age correlative magmatism also observed in the formerly along-strike orogens of Australia and Antarctica (e.g. Allibone et al., 1993; Cawood, 1984; Mortimer et al., 2017). In New Zealand, extensive work has been devoted to identifying and understanding the emplacement history and chemical evolution of several Early Paleozoic and Mesozoic suites, especially in the Fiordland region (e.g. Allibone et al., 2009; Allibone and Tulloch, 2004; Allibone et al., 2007; Decker et al., 2017; Kimbrough et al., 1994; Milan et al., 2017; Muir et al., 1994, 1996a; Muir et al., 1998; Muir et al., 1995; Muir et al., 1996b; Price et al., 2006; Schwartz et al., 2017; Scott and Palin, 2008; Tulloch et al., 2009; Turnbull et al., 2010; Waight et al., 1998a; Waight et al., 1998b). In contrast, the Late Permian to

1
2
3
4
5
6
7
8
9
10
11
12
13
14
15
16
17
18
19
20
21
22
23
24
25
26
27
28
29
30
31
32
33
34
35
36
37
38
39
40
41
42
43
44
45
46
47
48
49
50
51
52
53
54
55
56
57
58
59
60
61
62
63
64
65

70 Middle Triassic rocks of the Longwood Suite, the easternmost suite of the Median Batholith
71 have received relatively little attention (McCoy-West et al., 2014; Mortimer et al., 1999a),
72 with the main focus being on the platinum prospectivity of layered gabbros and peridotites
73 (Ashley et al., 2012; Mortimer et al., 2016; Price et al., 2006; Spandler et al., 2003; Spandler
74 et al., 2000). Of more interest is the fact the Longwood Suite records the re-initiation of
75 Median Batholith magmatism at the south Gondwana margin, after a c. 40 Ma pause, as the
76 result of a major tectonic reorganization.

77 In this contribution, we present new U-Pb zircon geochronology, trace element
78 systematics, Sr-Nd radiogenic isotope compositions and novel $^{146}\text{Nd}/^{144}\text{Nd}$ ratios of intrusive
79 rocks from the Foveaux Strait region of southern New Zealand. This combination of
80 radiogenic and stable isotopes allows constraints to be placed on both the sources of the
81 magmatism (i.e. mantle vs. crustal contributions), as well as deciphering magmatic processes
82 (obscured in conventional datasets) involved in their petrogenesis. Building on McCoy-West
83 et al. (2014), these new data refine and improve our knowledge of the time range and spatial
84 extent of the Permo-Triassic Longwood Suite of the Tuhua Intrusives. They affirm that, in
85 terms of geochemical and isotopic parameters, the Longwood Suite is distinctly more
86 primitive than older and younger plutonic suites of the Tuhua Intrusives. The Longwood
87 Suite therefore reflects a unique interplay between tectonics and magma genesis at the
88 Gondwana continental margin which enabled the generation of coeval primitive Na-rich
89 granitoids and layered gabbroids and peridotites.

90

91 **2.0 Geological Setting**

92 The Paleozoic to Mesozoic geological basement of New Zealand can be divided into two
93 principal components (Landis and Coombs, 1967; Mortimer, 2004; Mortimer et al., 2014): 1)

94 the Western Province which comprises Early Paleozoic terranes intruded by Early Paleozoic
 95 to Late Cretaceous Tuhua Intrusives plutons and batholiths; 2) the Eastern Province which
 96 comprises several Permian to Early Cretaceous terranes that represent crustal material
 97 accreted to the Gondwana margin from the Permian to Cretaceous. The focus of this paper is
 98 on the southeastern Tuhua Intrusives within the Median Batholith. The c. 10,200 km² Median
 99 Batholith lies along the eastern edge of the Western Province and its Cambrian to Early
 100 Cretaceous, composite regional arc-root plutonic complexes preserve a rich intrusive record
 101 of subduction related magmatism (Mortimer et al., 1999b). Our study area is the Foveaux
 102 Strait region in the southern part of the South Island (Fig. 1). Here, the Median Batholith is
 103 composed of two distinct suites: 1) the Longwood Suite (McCoy-West et al., 2014), of Late
 104 Permian to Middle Triassic (c. 261-245 Ma) plutonic rocks that vary from ultramafic to felsic
 105 in composition, with all analysed rocks possessing isotopically primitive characteristics
 106 (McCoy-West et al., 2014; Mortimer et al., 1999a; Nebel et al., 2007; Price et al., 2011; Price
 107 et al., 2006; Tulloch et al., 1999); and 2) the Darran Suite (Allibone et al., 2009), which
 108 consists of mainly Late Triassic to Early Cretaceous (c. 232-130 Ma) subduction-related I-
 109 type plutonic rocks (Allibone et al., 2009; Allibone and Tulloch, 2004; Buriticá et al., 2019;
 110 Kimbrough et al., 1994; McCoy-West et al., 2014; Mortimer et al., 1999a; Muir et al., 1998).
 111 To the east, the plutonic rocks of the Median Batholith intrude the Permian Brook Street
 112 Terrane (Fig. 1). Prior to the dating work of McCoy-West et al. (2014), the Permian plutons
 113 now classified as Longwood Suite were regarded as subvolcanic intrusions coeval with
 114 Brook Street Terrane magmatism, and/or all the Permian-Jurassic plutons along the
 115 Longwood coast were regarded as part of a single subduction-related, I-type batholithic
 116 complex (Price et al., 2011).

117 The Brook Street Terrane consists of mafic to intermediate volcanic and volcanoclastic
 118 rocks that are dominated by plagioclase- and clinopyroxene-phyric basalts, and can be

characterized, based on their major and trace element geochemistry, as being an island-arc tholeiitic suite (Houghton, 1981, 1985; Sivell and Rankin, 1983; Spandler et al., 2005). Recent interpretations of sedimentary and geochemical characteristics indicate that the Brook Street Terrane and the Gympie Terrane (an inferred along-strike Australian correlative) probably have some geological connection to the Gondwana margin (Adams et al., 2002; Li et al., 2015; Robertson and Palamakumbura, 2019), instead of having formed in an intra-oceanic setting with very limited input of continental material (Frost and Coombs, 1989; Houghton and Landis, 1989). The biostratigraphic age range of the Brook Street Terrane has most recently been assessed by Campbell (2019): all known Brook Street Volcanics Group fossil localities are Early Permian (c. 295-275 Ma), and the overlying, non-volcanic Productus Creek Group (Landis et al., 1999), a local but highly fossiliferous unit in the Takitimu Mountains (Fig. 1), is latest Early to Late Permian (c. 275-254 Ma).

The Longwood Suite, as first defined by McCoy-West et al. (2014), includes the isotopically primitive ($\epsilon^{143}\text{Nd}_{(t)} = \geq 5.4$; Mortimer et al., 1999a; Nebel et al., 2007; Price et al., 2006) Hekeia Gabbro and Pourakino Trondhjemite intrusions in the Longwood Range, along with plutonic rocks exposed near Oraka Point and on Bluff Peninsula (Fig. 2a-b; Challis and Lauder, 1977; Mortimer et al., 1999a; Price et al., 2006). Previous work has focused mainly on the distribution of rock types and elemental geochemistry, due to the platinum potential of the gabbros (Ashley et al., 2012; Cowden et al., 1990; Mossman, 1973; Spandler et al., 2003). Zircon geochronology confirms the Pourakino Trondhjemite (c. 261-252 Ma; McCoy-West et al., 2014; Tulloch et al., 1999) and Hekeia Gabbro (c. 258-252 Ma; McCoy-West et al., 2014) were emplaced essentially coevally although locally, trondhjemite dikes are seen to cut gabbro. Significant hornblende hornfels contact metamorphism and a sharp intrusive boundary between the volcanic Brook Street Terrane rocks and the aforementioned Longwood Suite plutonic rocks (Mortimer et al., 1999a; Service, 1937) suggests a significant

144 difference in age. The emplacement depth of the Pourakino Trondhjemite was c. 5-9 km
145 (Mortimer et al., 1999b).

146 The Darran Suite, consists of mainly Late Triassic to Early Cretaceous (c. 232-130 Ma)
147 subduction-related I-type plutonic rocks (Allibone et al., 2009). Darran Suite plutons (Fig. 1)
148 outcrop throughout eastern Fiordland, in the western Longwood Range, on the Longwood
149 coast, and in northern Stewart Island (Allibone et al., 2009; Allibone and Tulloch, 2004;
150 Kimbrough et al., 1994; McCoy-West et al., 2014; Mortimer et al., 1999a; Muir et al., 1998;
151 Scott and Palin, 2008; Williams and Harper, 1978). The Darran Suite can be distinguished
152 from the more voluminous and younger (c. 129-105 Ma) Separation Point Suite on the basis
153 of the lower Sr/Y of the granitoids (Tulloch and Kimbrough, 2003). Variations in radiogenic
154 isotope (Sr-Nd-Hf) compositions with time are also observed through the Darran and
155 Separation Point suites indicative of an increase in the influence of crustal sources in the
156 migrating Mesozoic subduction arc (Milan et al., 2017; Pickett and Wasserburg, 1989;
157 Schwartz et al., 2021; Turnbull et al., 2021).

158 Ruapuke Island (Fig. 2c) is a small (16 km²) low-lying island located between Bluff and
159 Stewart Island in the center of Foveaux Strait (Fig 1). Geologically it is poorly studied with
160 only reconnaissance mapping and petrography undertaken (Watters, 1978; Webster, 1981).
161 Both plutonic rocks and metavolcanic rocks outcrop on the island. The metavolcanic rocks are
162 dominated by hornblende hornfels comparable to those seen near Bluff and were mapped as
163 Brook Street Terrane by Turnbull and Allibone (2003). Across the island, a broader range of
164 plutonic rock types than seen near Bluff are observed. These include tonalite, trondhjemite,
165 hornblende gabbro, and gabbro-norite (Webster, 1981). The plutonic rocks of Ruapuke Island
166 have been suggested to be correlatives of either the Anglem Complex, Stewart Island (Watters,
167 1978) or the Bluff Intrusive Complex (Turnbull and Allibone, 2003). Prior to this work, the
168 only radiometric dating from Ruapuke Island was a K-Ar hornblende age of 222 Ma from a

quartz monzodiorite at South Point (Devereux et al., 1968; age recalculated using decay constants of Steiger and Jäger, 1977).

3.0 Analytical Techniques

A comprehensive description of the analytical techniques implemented herein can be found in the supplementary data, with a brief description provided here. Whole rock geochemistry was conducted at the Arthur Holmes Geochemistry Labs, Durham University. Following a conventional HF-HNO₃ digestion of 200 mg of powder, trace element concentrations were determined using 5 % of this material following established protocols (e.g. Ottley et al., 2003). Following spiking and equilibration with a ¹⁴⁵Nd–¹⁵⁰Nd double spike (McCoy-West et al., 2017; McCoy-West et al., 2020b), Nd and Sr were separated using well-established chromatographic techniques (e.g. Charlier et al., 2006; McCoy-West et al., 2016). Strontium and Nd isotope measurements were performed using a *Triton Plus* thermal ionization mass spectrometer in static collection mode. Stable Nd isotope ratios are expressed using conventional delta notation, where $\delta^{146}\text{Nd}$, is the per mil deviation in the measured ¹⁴⁶Nd/¹⁴⁴Nd relative to the widely measured reference standard JNdi-1. A distinct advantage of the Nd double spike approach implemented here is that it allows $\delta^{146}\text{Nd}$ and ¹⁴³Nd/¹⁴⁴Nd to be obtained simultaneously from a single measurement (see McCoy-West et al., 2020b for further details), therefore allowing constraints to be placed on both the source or age of a material and the processes involved in its formation. Zircon dating was undertaken at the Australian National University, using SHRIMP-RG and standard operating conditions (e.g. McCoy-West et al., 2014; Muir et al., 1996a). Briefly, Th/U and U/Pb ratios and Pb isotopic compositions were measured in a peak-stepped cycle. Uranium and Th concentrations were normalized using the SL13 zircon (Ireland and Williams, 2003) and U/Pb was normalized using the Temora2 zircon

(Black et al., 2003). Common Pb was removed through projecting to the Concordia (^{207}Pb correction method of Muir et al., 1996a).

4.0 Results

4.1 *SHRIMP geochronology*

The calculated common Pb corrected ^{206}Pb - ^{238}U weighted mean ages of four zircon bearing samples are summarized in Table 1, with the complete U-Th-Pb isotopic compositions presented in Supplementary Data, Table S1. Cathodoluminescence images show that zircon morphology is dependent on the bulk rock composition with the mafic samples containing subhedral to anhedral zircons that display irregular banding or weak zonation (Supplementary Data, Fig. S1 a, c), whereas the more felsic samples contain euhedral to subhedral, predominantly sector zoned zircons (Supplementary Data, Fig. S1 b, d). In all the samples the zircons are relatively coarse grained (c. 100-400 μm) and represent a single igneous crystallization episode with no inherited cores observed. Isotopic compositions are shown graphically in the form of Tera-Wasserburg concordia diagrams in Figure 3 (Tera and Wasserburg, 1972). All mean ages of the zircon populations are reported with propagated two sigma uncertainties.

A gabbroic dike (P82432) crosscutting the Greenhills Complex ultramafic rocks northwest of Bluff, has a calculated ^{206}Pb - ^{238}U mean age of 256.0 ± 1.8 Ma (Fig. 3a). Three zircon bearing samples from Ruapuke Island have mean ages varying from c. 259 to 243 Ma, with the crystallization ages becoming younger to the south (Fig. 2c). A hornblende diorite (P32769) from North Head has a calculated ^{206}Pb - ^{238}U mean age of 258.5 ± 2.8 Ma; a single analysis with an older concordant age of 289 ± 7 Ma is excluded from the calculated mean (Supplementary Data, Table S1; Fig 3b). A tonalite (OU38374) from the middle of Ruapuke

Island has a ^{206}Pb - ^{238}U mean age of 247.8 ± 2.7 Ma. A diorite (OU38336) collected near West Point has a U-Pb mean age of 243.2 ± 2.4 Ma (two analyses with significantly younger ^{206}Pb - ^{238}U ages that do not fall onto a mixing line with common Pb, were excluded due to minor Pb loss; Fig. 3c). In all cases the calculated mean ages are within uncertainty of the concordia ages (Fig. 3). Within uncertainty, these new ages fall within the range of previously published crystallization ages of c. 261 to 245 Ma from the Longwood Suite as defined in the nearby Longwood Range (McCoy-West et al., 2014; Price et al., 2006; Tulloch et al., 1999).

4.2 Major and trace element geochemistry

Major and trace element compositions of the igneous rocks investigated here are presented in Supplementary Data, Table S2. Previous work has shown that Brook Street Terrane igneous rocks are dominated by primitive basaltic and basaltic andesites ($\text{SiO}_2 = 50.7 \pm 3.9$ wt % and $\text{MgO} = 6.2 \pm 2.4$ wt % (1 s.d.); $n = 70$; Nebel et al., 2007; Robertson and Palamakumbura, 2019; Spandler et al., 2005). Our new trace element analyses confirm that Brook Street Terrane amphibolite and granofels samples from Ruapuke Island have similar compositions to these (Fig. 4). They all display moderate enrichment relative to chondrites ($\text{Ce}_{\text{(N)}} = 9\text{-}34$) but possess flat chondrite normalized REE patterns ($\text{La}/\text{Yb}_{\text{(N)}} = 0.83\text{-}1.47$; Fig. 4a). Primitive-mantle-normalized multi-element diagrams have positive U, Pb and Sr anomalies with strong negative depletion Nb, and Zr-Hf (Fig. 4b).

Reference samples of the Pourakino Trondhjemite of the Longwood Suite in the Longwood Range are dominated by plagioclase and quartz with (by definition) minimal alkali feldspar (Supplementary Data, Fig. S2a), whereas the younger Hollyburn Intrusives (Darran Suite) have notably higher ratios of alkali feldspar to plagioclase. Another way of showing the same thing is on an anorthite-albite-orthoclase normative diagram (Supplementary Data, Fig. S2b), in which the Pourakino Trondhjemite (Longwood Suite) is

dominated by orthoclase-poor trondhjemites and tonalites, and the Darran Suite by more orthoclase-rich granodiorites and granites. On Ruapuke Island both orthoclase-poor and -rich compositions exist, indicating that both plutonic suites are present.

Trondhjemitic and gabbroic Longwood Suite reference samples from the Longwood Range both possess relatively flat REE element patterns ($\text{La/Yb}_{(N)} = 0.37\text{--}3.8$; Fig. 4c) that vary from slightly depleted to slightly enriched in LREE ($\text{La/Sm}_{(N)} = 0.23\text{--}3.1$). Most samples also possess flat middle(M) REE to heavy(H) REE ($\text{Gd/Yb}_{(N)} = 1.2\text{--}1.8$), except sample P81173 a trondhjemite dike which has a convex REE pattern ($\text{Gd/Yb}_{(N)} = 0.77$; Fig. 4c). Multielement patterns of these samples are highly variable due to their major element composition (i.e. $\text{SiO}_2 = 45\text{--}74$ wt. %) and possibly also due to variable crystal accumulation in some gabbros, but most show negative depletion of Zr-Hf and Nb, and positive Pb and Sr anomalies (Fig. 4d), again P81173 is anomalous with a strong positive Hf not seen in the other samples. The samples from Ruapuke Island analysed here possess similar compositions to Longwood Suite rocks with relatively flat REE patterns ($\text{La/Yb}_{(N)} = 18$; Fig. 4e), and unremarkable multielement patterns, although clear negative Zr-Hf depletions are observed in all samples (Fig. 4f). To compare Longwood Suite with older Tuhua Intrusives suites, we analysed a sample of Riwaka granite (c. 364 Ma, Devonian) from the northern South Island (Turnbull et al., 2017). The Riwaka Granite is different in that it is LREE enriched ($\text{La/Yb}_{(N)} = 18$; Fig. 4e) and displays large enrichments in a range of very incompatible elements (e.g. Rb, U, Th; Fig. 4f).

4.3 Radiogenic Sr-Nd isotopes

Isotopic compositions of 17 samples are presented in Table 2. New analyses of plutons and dikes from the Hekeia Gabbro and Pourakino Trondhjemite all have primitive isotope compositions with unradiogenic $^{87}\text{Sr}/^{86}\text{Sr}_{(t)}$ of < 0.7033 and radiogenic $\epsilon^{143}\text{Nd}_{(t)} > +6$ (Fig. 5), consistent with previous analyses of the Longwood Suite in the same area (Mortimer et al.,

1999a; Price et al., 2006; Tulloch et al., 1999). The dike from the Greenhills Intrusive Complex (P82432) dated here at 256.0 ± 1.8 Ma also has an isotope composition ($^{87}\text{Sr}/^{86}\text{Sr}_{(t)} = 0.7032$; $\epsilon^{143}\text{Nd}_{(t)} = +8.0\text{--}8.2$) that matches other Longwood Suite rocks. Four samples from Ruapuke Island, which vary from gabbroic to tonalitic, present comparable unradiogenic Sr and radiogenic Nd ($^{87}\text{Sr}/^{86}\text{Sr}_{(t)} = 0.7029\text{--}0.7032$; $\epsilon^{143}\text{Nd}_{(t)} = +6.3\text{--}7.7$). Combined with the U-Pb ages, the Sr and Nd isotope data establish an important correlation of these Ruapuke Island plutons to the Longwood Suite (Fig. 6). The Riwaka Granite has significantly more radiogenic Sr and unradiogenic Nd ($^{87}\text{Sr}/^{86}\text{Sr} = 0.7095$; $\epsilon^{143}\text{Nd} = -3.1$ to -3.3) than Longwood Suite magmas, instead being closer in composition to the older Devonian-Carboniferous magmatic suites (Supplementary Data, Fig. S3; Muir et al., 1998; Muir et al., 1996b; Tulloch et al., 2009).

Our new samples of Brook Street Terrane in southern South Island possess radiogenic $\epsilon^{143}\text{Nd}_{(t)} > +6$, in agreement with previous analyses (Fig. 6; Adams et al., 2005; Frost and Coombs, 1989; Nebel et al., 2007), and generally unradiogenic $^{87}\text{Sr}/^{86}\text{Sr}_{(t)}$ of <0.7033 , although two of the samples display more radiogenic Sr compositions (P84061: $^{87}\text{Sr}/^{86}\text{Sr}_{(t)} = 0.7037$; P32787: $^{87}\text{Sr}/^{86}\text{Sr}_{(t)} = 0.7044$). The samples from Ruapuke Island also show primitive isotope compositions with $^{87}\text{Sr}/^{86}\text{Sr}_{(t)} < 0.7030$ and $\epsilon^{143}\text{Nd}_{(t)} > +8$ (Fig. 5).

4.4 Stable Nd isotopes

No correlations are observed between $\delta^{146}\text{Nd}$ and either Nd concentration or $^{143}\text{Nd}/^{144}\text{Nd}$ (Supplementary Data, Fig. S4). Samples of Brook Street Terrane from both the southern South Island and Ruapuke Island possess a restricted range of $\delta^{146}\text{Nd}$ from -0.053 ‰ to -0.027 ‰ ($\delta^{146}\text{Nd} = 26$ ppm), despite possessing a wide range of Nd concentrations from 6.1 to 18.8 ppm (Supplementary Data, Fig. S4; Table 2). This range is comparable with previously measured $\delta^{146}\text{Nd}$ compositions of basaltic igneous rocks (Fig. 7; McCoy-West et al., 2021; McCoy-West et al., 2017, 2020a; McCoy-West et al., 2020b) and within

uncertainty of the average composition of bulk silicate Earth ($\delta^{146}\text{Nd} = -0.024 \pm 0.031 \text{ ‰}$; McCoy-West et al., 2021). The plutonic rocks from Ruapuke Island also possess a restricted range of $\delta^{146}\text{Nd}$ with values from -0.051 ‰ to -0.015 ‰ ($\delta^{146}\text{Nd} = 36 \text{ ppm}$; Fig. 6). Nd stable isotope compositions of samples in the Longwood Suite are significantly more variable with $\delta^{146}\text{Nd}$ ranging from -0.075 ‰ to $+0.158 \text{ ‰}$ ($\delta^{146}\text{Nd} = 223 \text{ ppm}$; Fig. 6), although most of this variability is restricted to samples with low Nd concentrations $< 2.8 \text{ ppm}$ (Supplementary Data, Fig. S4). Two notable samples are a Pourakino Trondhjemite dike sample (P81173: $\delta^{146}\text{Nd} = 0.149 \pm 0.023 \text{ ‰}$; $n = 2$) and Hekeia Gabbro sample (P82430: $\delta^{146}\text{Nd} = 0.057 \pm 0.023 \text{ ‰}$; $n = 2$), with the former possessing the heaviest $\delta^{146}\text{Nd}$ observed so far in terrestrial magmatic rocks. Large fractionations in $\delta^{146}\text{Nd}$ are observed at both high and low Mg# and SiO_2 contents (Fig. 7). While samples with low P_2O_5 contents ($< 0.08 \text{ wt } \%$) generally display variations from the bulk silicate Earth $\delta^{146}\text{Nd}$ composition (Fig. 7c).

5.0 Discussion

5.1 Ruapuke Island geology

Despite its small 16 km^2 size, Ruapuke Island has a complex geologic history (Webster, 1981), with rocks spanning at least c. 60 Ma (this study). Like the Longwood Range and Bluff area, it is one of the few places in New Zealand where an unfaulted intrusive boundary between the Brook Street Terrane and Median Batholith is exposed. Metavolcanic hornblende hornfels rocks correlated with Greenhills Group (Brook Street Terrane) outcrop on the eastern side of Ruapuke Island, with a widespread intermingled zone (up to 1 km wide) where the leucotonalite that dominates the island intrudes the hornblende hornfels (Fig. 2c; Webster, 1981). Two samples of the hornblende hornfels show isotope compositions more primitive than Longwood Suite with $^{87}\text{Sr}/^{86}\text{Sr}_{(t)} = 0.7028\text{--}0.7029$ and $\epsilon^{143}\text{Nd}_{(t)} = +8.5$ confirming their links to the broader Brook Street Terrane (Table 2; Fig. 5). As mapped by

Webster (1981), the majority of Ruapuke Island is dominated by tonalite, a sample of which we have U-Pb dated at 247.8 ± 2.7 Ma (Table 1; Fig. 3). Two more mafic plutons from the coast of Ruapuke Island are older and younger, with a hornblende gabbro from North Head dated at 258.5 ± 3.0 Ma (which is with uncertainty of magmatism in the Bluff Intrusive Complex), and a diorite from West Point dated at 243.2 ± 2.5 Ma (Fig. 2c). These samples also possess unradiogenic Sr and radiogenic Nd ($^{87}\text{Sr}/^{86}\text{Sr}_{(t)} < 0.7033$; $\epsilon^{143}\text{Nd}_{(t)} > +6.3$) comparable compositions to Longwood Suite samples from the mainland and are now included in this suite based on their age and isotopic similarity. A geochemically distinct quartz monzodiorite outcrops in the southern portion of the Ruapuke Island (Fig. 2c), and gave the aforementioned K-Ar hornblende age of 222 Ma. It also has a distinctly lower $\epsilon^{143}\text{Nd}_{(t)}$ of +4.2 (Tulloch, 2001) than rocks of the Longwood Suite. Both the 222 Ma age (which we interpret as approximating an unreset cooling age) and geochemistry confirm it is part of the Darran Suite (Fig. S2 and see section 5.3 for further discussion). The four dated samples from Ruapuke Island varying from c. 259 to c. 222 Ma, and become progressively younger to the south (Fig. 2c). This age progression is comparable to what is observed from east to west in the Longwood Range and nearby coast (see Figure 2 in McCoy-West et al., 2014), although the Longwood Range has been rotated due to the large scale regional deformation of New Zealand's lithostratigraphic terranes associated with oroclinal bending (Mortimer, 2014; see Figs. 1 or 8).

5.2 Improved understanding of the timing and extent of the Longwood Suite

Despite the protracted history of the Median Batholith (c. 495-105 Ma), the Longwood Suite is unique in that it possesses primitive Sr-Nd isotope compositions (Fig. 5; $^{87}\text{Sr}/^{86}\text{Sr}_{(t)} = \leq 0.7033$; $\epsilon^{143}\text{Nd}_{(t)} = \geq 5.4$) combined with radiogenic $^{176}\text{Hf}/^{177}\text{Hf}$ (Nebel et al. 2007), which

reflects direct extraction from the mantle with limited or no input (contamination) from
crustal reservoirs. In this respect it differs from both older and younger plutonic suites (Fig.
9) that spatially, lie within the outcrop envelope of the Median Batholith further to the south
and west (e.g. Stewart Island and Fiordland see Fig. 1). As originally defined, the Longwood
Suite (McCoy-West et al., 2014) included the Late Permian to Middle Triassic (c. 261-245
Ma) isotopically primitive plutonic bodies (e.g. Hekeia Gabbro and Pourakino Trondhjemite;
Fig. 2) in the Longwood Range, as well plutons of comparable age of the Bluff Intrusive
Complex. A gabbroic dike (P82432) from the Greenhills Intrusion, Bluff Intrusive Complex,
dated here at 256.0 ± 1.8 Ma, agrees within uncertainty with previous ages of the nearby Flat
Hills Intrusion of 256.3 ± 4.0 Ma (^{238}U - ^{206}Pb bulk age; Kimbrough et al., 1992) and $259.1 \pm$
 4.4 Ma (Price et al., 2006). Furthermore, the Sr-Nd isotope composition of this sample
($^{87}\text{Sr}/^{86}\text{Sr}_{(t)} = 0.7032$; $\epsilon^{143}\text{Nd}_{(t)} = 8.0$ - 8.2) confirms for the first time an isotopic as well as age
correlation between these distinct plutonic bodies in Longwood Range and Bluff areas (≥ 30
km apart). Despite considerable geochemical ($\text{SiO}_2 = 47.9$ to 63.7 wt %) and lithologic
variability (gabbro to leucotonalite), all of the Ruapuke samples analysed possess primitive
Sr-Nd isotope compositions (Fig. 5; $^{87}\text{Sr}/^{86}\text{Sr}_{(t)} = 0.7029$ - 0.7032 ; $\epsilon^{143}\text{Nd}_{(t)} = 6.3$ - 7.7),
confirming their association with the Longwood Suite. The three dated plutonic rocks from
Ruapuke Island have U-Pb zircon crystallization ages ranging from 258.5 ± 3.0 Ma to 243.2
 ± 2.5 Ma (Table 1; Fig. 3), which are comparable to, but extend to a slightly younger age,
than the existing geochronology of the Longwood Suite (McCoy-West et al., 2014; Mortimer
et al., 1999a; Price et al., 2006; Tulloch et al., 1999). Consequently, we now propose an age
range of c. 261-243 Ma for the Longwood Suite. The inclusion of samples from Ruapuke
Island slightly broadens the extent of the Longwood Suite plutonism in both time (c. 2 Ma)
and space, with the outcrop strike length of the Longwood Suite now c. 25 km further
southeast (Fig. 8). Although this may seem a minor point, in this paper we have increased the

number of dated Longwood Suite samples by c. 40 %, and those with isotopic fingerprinting by c. 56 %. Further afield, and as discussed below (Section 5.7), Permian to Triassic I-type plutonic rocks of the New England Orogen, Australia may be related (e.g. Bryant et al., 1997).

5.3 Distinguishing the Longwood and Darran suites

The complexity of the Median Batholith, where multiple episodes of plutonism occur in close proximity, means that both age and geochemical relationships are used to define plutonic suites (e.g. Allibone et al., 2009; Tulloch et al., 2009). Samples from the Longwood and Darran suites are present in the inland Longwood Range, along the Longwood coast and on Ruapuke Island (Fig. 2). Furthermore, the ages of the two suites (see Fig. 8b and Supplementary Data, Fig. S5) are only locally separated by c. 11 Ma (243.2 ± 2.4 to 232 ± 1.5 Ma; herein and McCoy-West et al., 2014, respectively) and by only c. 4 Ma if the 238.7 ± 2.4 Ma Mt. Edgar Diorite Darran Suite age of Ringwood et al. (2021) is used. The Longwood Suite ($\epsilon^{143}\text{Nd}_{(t)} = +6.78 \pm 1.46$; 2 s.d. $n = 31$) can be easily distinguished from the Darran Suite ($\epsilon^{143}\text{Nd}_{(t)} = +3.68 \pm 1.33$; 2 s.d. $n = 38$) based on their distinct radiogenic Nd isotope compositions (Fig. 10a). However, isotopic analyses are only available for a small proportion of samples, so we have investigated a range of other geochemical criteria, which can be used to distinguish Longwood from Darran rocks. Longwood Suite samples have distinctive flat REE patterns (Fig. 4) and at comparable SiO_2 have lower $\text{La}/\text{Sm}_{(N)}$ than samples from the Darran Suite (Fig. 10b). When focussing only on granitoids ($\text{SiO}_2 \geq 64$ wt %) the Longwood samples have significantly lower K/Na (≤ 0.4 ; Fig. 10c) and Rb (≤ 10 ; Fig. 10d) than Darran rocks with similar SiO_2 . Interestingly, the Longwood Suite samples also possess distinctive low Nb/Ta (≤ 5 ; $n = 6$), which is not observed elsewhere in the plutonic record of the Median Batholith (Fig. 9d). Another widely used parameter to distinguish between plutonic suites is

Sr/Y (e.g. Allibone et al., 2007; Tulloch and Kimbrough, 2003), which has been taken as being indicative of the depth of melting (i.e. high Sr/Y is consistent with a deeper garnet bearing melting region; Moyen, 2011). Although extremely variable (Fig. 9b: note the log scale), most granitoids from the younger Separation Point Suite are dominated by high Sr/Y (≥ 40 after Drummond and Defant, 1990) with a median Sr/Y of 125 (Sr/Y = 11-829; n = 112), whereas most Darran Suite granitoids have significant lower Sr/Y with an median value of 24 (Sr/Y = 2-329; n = 105). The high-Na granitoids of the Longwood Suite appear intermediate between these two suites with Sr/Y ranging from 39 to 342 and a median value of 76 (n = 18; Fig. 9b). This excludes the chemically distinct high-K (K/Na > 1.5) Oraka Point granites that have significantly lower Sr/Y values of 8-9 (n = 2).

Previous researchers have used Sr/Y to calculate crustal thickness (e.g. Chapman et al., 2015; Profeta et al., 2015), however, the observation of intermediate Sr/Y in the Longwood Suite suggests this parameter is not always a reliable proxy for melting depth. As well as their intermediate Sr/Y Longwood Suite magmas also possess very low La/Yb_(N) < 10, and significantly flatter REE patterns than comparable rocks in the Darran Suite (Fig. 4c and 10b) and Tuhua Intrusives (Fig. 9c). When calculating crustal thickness (after Profeta et al., 2015 using rocks with SiO₂ = 55 to 68 wt %) based on median La/Yb_(N) and Sr/Y results in disparate crustal thickness estimates of c. 27 km and > 60 km, respectively. Mantle and Collins (2008) tracked Ce/Y in basaltic samples through time in New Zealand to reconstruct Moho depth (see Figure 3 therein), with the results suggesting a minimum in crustal thickness of <25 km around 260 Ma, which agrees much better with the La/Yb_(N) crustal thickness estimate. Aluminium in hornblende geobarometry by Mortimer et al. (1999a) indicated Pourakino Trondhjemite emplacement depths of 5-9 km. Therefore, we advocate caution when applying Sr/Y in isolation to reconstruct crustal thickness.

5.4 Using Stable Nd isotopes to constrain magmatic petrogenesis

Unlike radiogenic isotope systems, stable isotope compositions are time-independent tracers of the processes a sample has experienced and thus may provide unique insights into the petrogenesis of igneous rocks (e.g. Dauphas et al., 2009; McCoy-West et al., 2019; Savage et al., 2011). Due to its high molar mass, and monovalent nature at magmatic temperatures, fractionations of Nd stable isotopes would be predicted to be small. Although the application of Nd stable isotopes remains in its infancy, resolvable fractionations in igneous rocks are widespread (McCoy-West et al., 2021; McCoy-West et al., 2017, 2020a; McCoy-West et al., 2020b). A global compilation of magmatic rocks including mid-ocean ridge, ocean island and island arc basalts possess Nd stable isotope compositions from -0.061‰ to $+0.022\text{‰}$ ($\delta^{146}\text{Nd} = 83\text{ ppm}$), with the average composition of the bulk silicate Earth calculated as $\delta^{146}\text{Nd} = -0.024 \pm 0.031\text{‰}$ (2 s.d.; $n = 80$; McCoy-West et al., 2021). The Brook Street Terrane consists of basaltic volcanic and volcanoclastic rocks (e.g. Frost and Coombs, 1989; Spandler et al., 2005), all measured samples possess a restricted range of $\delta^{146}\text{Nd}$ from -0.053‰ to -0.027‰ ($\delta^{146}\text{Nd} = 26\text{ ppm}$; $n = 6$; Fig. 6), which is indistinguishable from the composition of the bulk silicate Earth. The relatively invariant $\delta^{146}\text{Nd}$ composition of these basaltic metasediments (i.e. hornfels) is consistent with contact metamorphism having had no resolvable effect on their Nd stable isotope compositions.

In contrast, the plutonic rocks of the Longwood Suite are significantly more variable with $\delta^{146}\text{Nd}$ ranging from -0.075‰ to $+0.158\text{‰}$ ($\delta^{146}\text{Nd} = 223\text{ ppm}$; $n = 10$; Fig. 6). This range is substantially larger than that seen previously in plutonic rocks ($\delta^{146}\text{Nd} = 44\text{ ppm}$; McCoy-West et al., 2017) or oceanic gabbros from Hole 735B which, although variable, extend towards isotopically light compositions (i.e. to -0.127‰ ; $\delta^{146}\text{Nd} = 101\text{ ppm}$; Fig. 6). Due to the incompatible nature of Nd in the dominate silicate phases involved in mafic magmatic processes ($D_{\text{Nd}} \leq 0.01$ to 0.4 ; McCoy-West et al., 2021), no resolvable effects of magmatic

differentiation (between 50 and 70 wt % SiO₂) are observed on Nd stable isotope compositions (McCoy-West et al., 2021; McCoy-West et al., 2017, 2020a). Instead the light $\delta^{146}\text{Nd}$ values observed in the oceanic gabbros were attributed to kinetic isotope fractionation, as the result of diffusion across disequilibrium boundaries, during repeated melt migration through the oceanic crust (McCoy-West et al., 2020a). No petrologic evidence exists for repeated melt percolation in the Longwood Suite rocks. However, the crystallization of REE-bearing accessory phases (e.g. monazite, allanite, xenotime, titanite or apatite), which can incorporate significant concentrations of LREE (up to 1000 fold enrichment; Exley, 1980; Hoskin, 2000) could generate stable isotope fractionations as suggested previously (McCoy-West et al., 2017; McCoy-West et al., 2020b). The crystallization of monazite, or other trace phases, is predicted to preferentially sequester light Nd isotopes, due to the effect of variations in Nd coordination environment between the accessory minerals and silicate melt. In the Longwood Suite rocks, larger fractionations of $\delta^{146}\text{Nd}$ from the composition of the bulk silicate Earth are observed in both the most primitive and evolved plutonic rocks (e.g. low and high SiO₂ and Mg#; Fig. 7), however, all samples with variable $\delta^{146}\text{Nd}$ have low P₂O₅ contents (< 0.08 wt %; Fig. 7c), which is reflective of the prior removal of phosphate minerals. For example, the heaviest sample (P81173; $\delta^{146}\text{Nd} = +0.158$ ‰) is a highly evolved (SiO₂ > 74 wt %) narrow trondhjemite dike with very low P₂O₅ (0.02 wt %), hence we infer that the crystallization and settling of monazite ([Ce,La,Nd,Th]PO₄) in the primary magma chamber, would leave the residual melt isotopically heavy explaining the dike's composition. In exploring such fractionation processes, geochemistry is a better tool than modal petrography; monazite is only ever an accessory phase and would, in the case of P81173, have been removed prior to crystallization of the trondhjemite. Further investigations of comagmatic samples that fractionate REE-bearing accessory minerals are clearly warranted.

5.5 Magmatic flux rates

The rate and duration over which new cogenetic material is added to a magmatic arc ultimately has implications for the tectonic processes that generated the magmas (e.g. Milan et al., 2017; Paterson et al., 2011). Calculations of the volume addition and flux rates of plutons and suites are highly dependent on, and vulnerable to, assumptions on age range, areal extent and intrusive depth. Nonetheless, we here make areal addition rate estimates for the Longwood Suite (Table 3), based on mapped areas of plutons and their ages (Mortimer et al., 2016; Turnbull and Allibone, 2003; this study). Note that we use areal addition rates (km^2/Ma) not the more speculative volume addition rates (km^3/Ma) which make assumptions on crustal thickness and vertical pluton extent. In the inland Longwood Range and nearby coast, the 258-245 Ma Hekeia Gabbro is c. 99 km^2 in area, the 261-253 Ma Pourakino Trondhjemite 65 km^2 , and the 232-203 Ma Darran Suite plutons 83 km^2 (Fig. 2a). Taken at face value, these GIS-calculated areas and age ranges give areal addition rates of $10 \text{ km}^2/\text{Ma}$ and $3 \text{ km}^2/\text{Ma}$ for Longwood and Darran suites, respectively. Further afield, the 24 km^2 Bluff Intrusive Complex is almost all gabbroic and peridotitic (Fig. 2b). Ruapuke Island is dominated by 10.9 km^2 of Longwood Suite granitoids, with a further c. 1.1 km^2 of Longwood Suite gabbroids and only 0.7 km^2 of Darran Suite rocks (Fig. 2c). Applying the wider age range of 261-243 Ma (= 18 Ma) to the wider (but still onland area) of 201 km^2 gives an areal addition rate of $11 \text{ km}^2/\text{Ma}$ for the entire onland Longwood Suite as presently known. However, the presence of semi-continuous positive magnetic anomalies in Foveaux Strait (Thomson Aviation, 2020) can be used to infer a greater undersea areal extent of the Longwood Suite between the Longwoods and Ruapuke Island, perhaps c. 770 km^2 which would yield an areal addition rate as high as $43 \text{ km}^2/\text{Ma}$. In Fiordland, areal addition rates of $67 \text{ km}^2/\text{Ma}$, and $105\text{--}375 \text{ km}^2/\text{Ma}$ have been calculated for the 167-127 Ma part of the Darran Suite and the 125-115 Ma Separation Point Suite, respectively (Milan et al., 2017).

Notwithstanding the uncertainties in these calculations, they demonstrate that the Longwood Suite is in fact a very low flux event for this portion of the Gondwana margin.

5.6 Trondhjemite petrogenesis

The Longwood Suite preserves the coeval emplacement of primitive ultramafic-mafic and felsic plutons. Bimodal magmatism is usually a feature of extensional and/or rift tectonic settings and is generally absent in convergent margin magmatism (e.g. Wilson, 1989). As shown in Figure 6 of Mortimer et al. (1999a), Hekeia Gabbro plagioclase and olivine compositions are broadly similar to those in other gabbros from global arc cumulates. The trace element composition of the Pourakino Trondhjemite are also comparable to those of global arc granitoids (i.e. Fig. 10d). Price et al. (2011) strongly emphasized the I-type nature of the Permian and Triassic Longwood and Darran suites along the Longwood coast.

Longwood Suite plutons possess extremely primitive radiogenic isotope compositions indicative of extraction from the mantle with limited to no crustal input ($\epsilon^{143}\text{Nd}_{(t)} > +5.5$; $^{87}\text{Sr}/^{86}\text{Sr}_{(t)} < 0.7032$; Fig. 5). However, the low Mg-number ($\text{Mg}\# \leq 0.35$) and Ni concentrations (≤ 10 ppm) of the Pourakino Trondhjemite, which are not in equilibrium with the mantle, confirm these melts do not represent direct extraction from the mantle. This characteristic is consistent with the well-established paradigm that trondhjemites are generated by partial melting of metamorphosed mafic rocks (e.g. Barker and Arth, 1976). It is noteworthy that the Pourakino Trondhjemite is 40 % by area of the Longwood Suite, thus a large volume of mafic protolith would have needed to have partially melted to yield such a large pluton. Similar to most other Phanerozoic trondhjemites (Tate et al., 1999; Wolf and Wyllie, 1994), the Pourakino Trondhjemite possesses extremely flat REE patterns (e.g. $\text{La}/\text{Yb}_\text{N} < 10$; $\text{La}/\text{Sm}_\text{N} < 5$; see Fig. 4) consistent with shallow melting in the absence of

residual garnet (Bryant et al., 1997; Gromet and Silver, 1987). Although the presence of garnet will be composition dependent, dehydration melting experiments are consistently garnet absent at < 0.8 GPa (c. 28 km; Rapp et al., 1991; Rushmer, 1991). Another striking feature of the Pourakino Trondhjemite is the distinctive low Nb/Ta ≤ 5 seemingly caused by low Nb values (Fig. 9). Due to their comparable geochemical behaviour, the fractionation of Nb from Ta during magmatic differentiation is unlikely and thus is probably a magma source signature. Experimental work has demonstrated that Nb/Ta fractionation is possible when residual (paragastic) amphibole is present in the melting region (Li et al., 2017; Tiepolo et al., 2001). Alternatively, the low Nb/Ta could be inherited directly from the precursor (Rapp et al., 2003), although most samples of the Brook Street Terrane possess near-chondritic Nb/Ta with only a few samples having low Nb/Ta < 5 (3/18; this paper and Spandler et al., 2005), making melting in the amphibole stability field the most likely scenario. All of the aforementioned geochemical characteristics, in combination with a shallow Moho at 260 Ma (Mantle and Collins, 2008), are consistent with generation of the Pourakino Trondhjemite by shallow melting (< 28 km) of an amphibolitic residue at the base of a thinned lithosphere.

5.7 Gondwana margin correlations and tectonic model

Permian and Triassic intrusions are also present along strike from the South Island (see Fig. 11) in the New England Orogen of eastern Australia (Cawood et al., 2011a; Cawood, 1984; Donchak et al., 2013; Rosenbaum, 2018). Early Permian (c. 295-280 Ma) New England granitoids are mainly S-type (Shaw et al., 2011) and are deformed around an oroclinal bend in the orogen (Bryant et al., 1997; Cawood et al., 2011b; Jessop et al., 2019). In contrast, Middle Permian to Middle Triassic (c. 270-235 Ma) granitoids, including the Clarence River Supersuite of Shaw and Flood (1981) form post-bending linear belts that were

538 intruded during a protracted compression phase (c. 270-260 Ma) of the Hunter-Bowen
 539 orogeny, part of the broader Gondwanide Orogeny (Cawood et al., 2011a; Cawood, 2005;
 540 Jessop et al., 2019). Some (but not all) of the Clarence River Supersuite plutons possess
 541 zircons with exceptionally primitive mantle-like $\varepsilon^{176}\text{Hf}$ values (Kemp et al., 2009; Shaw et
 542 al., 2011), which are correlated with their whole rock Sr-Nd isotope compositions (up to
 543 $\varepsilon^{143}\text{Nd} = +6$; Bryant et al., 1997; Hensel et al., 1985). This pulse of primitive east Australian
 544 magmatism is analogous to that observed in Zealandia. Mortimer et al. (2011) also noted that
 545 the platinum prospectivity of the layered Hekeia Gabbro was shared by some Late Permian to
 546 Middle Triassic layered mafic intrusions (Fig. 11b) in the northern New England orogen (e.g.
 547 Wateranga (244 Ma), Eulogie Park and Bucknalla intrusions; Donchak et al., 2013; Talusani
 548 et al., 2005). Additional evidence of mantle-dominated magmatism relatively uncontaminated
 549 by continental crust or lithosphere is seen in other geochemical datasets of the Permian
 550 Gondwana margin. These include the distinctive low Ce/Y ratios in basaltic and gabbroic
 551 rocks (Mantle and Collins, 2008), a c. 247 Ma granodiorite with $\varepsilon^{143}\text{Nd}_{(t)} = 6.4$ from the West
 552 Norfolk Ridge (Mortimer et al., 1998), and elevated $\varepsilon^{176}\text{Hf}$ seen in detrital zircons shed from
 553 the Gondwana margin (Campbell et al., 2020; Nelson and Cottle, 2017). All of these datasets,
 554 as well as the aforementioned characteristics of the New Zealand and Australian plutons,
 555 indicate that Gondwanan rocks and zircons of pre- and post-Permian age are isotopically less
 556 primitive than those of Permian age.

557 Based on these studies and our own observations we propose a mechanism whereby, in
 558 the Permian, pre-existing Gondwana subcontinental lithospheric mantle was replaced by crust
 559 and mantle of the Brook Street Terrane, and its Australian equivalent, the Gympie Terrane
 560 (Fig. 11a). This Early Permian time interval (c. 300-260 Ma) corresponds to an episode of
 561 inferred transpression, oroclinal bending, terrane accretion and stepping out of the continent-
 562 ocean boundary in the New England orogen (Cawood et al., 2011b; Rosenbaum, 2018;

Veevers, 2004). As revealed in Figure 8, it was also a pronounced magmatic lull or gap in the Median Batholith (Zealandia part of Gondwana). That a period of seemingly no plutonism was preceded by the A-type Foulwind Suite (Tulloch et al., 2009) suggests that the Zealandia segment of Gondwana, was not necessarily a convergent margin during that interval but that it lay offshore, east of a parautochthonous Gympie-Brook Street arc (e.g. Li et al., 2015; Robertson and Palamakumbura, 2019). From the Late Permian (c. 260 Ma) onwards a new, convergent, phase of Gondwana margin development began (Fig. 11b). We propose that this convergence caused tectonic underplating of the Brook Street Terrane and Gympie Terrane mafic arc crust and underlying mantle under the Gondwana margin. Melting of the underplated mantle would have given rise to the Hekeia Gabbro, and melting of the underplated mafic crust would produce the Pourakino Trondhjemite. The Late Permian Productus Creek Group of the Brook Street Terrane was still being deposited in the early stages of the underplating (Fig. 11b). The new Late Permian-Middle Triassic magmatic arc was emplaced across the previously formed oroclinal bend and was broadly co-eval with the compressional Hunter-Bowen Orogeny (Cawood et al., 2011b; Rosenbaum, 2018). The isotopically primitive, largely bimodal plutonism of the Longwood Suite was relatively short-lived and, as the magmatic arc matured, migrated, and thickened, became supplanted by more ‘normal’ gabbro-diorite-granodiorite-granite Darran Suite magmatism.

5.8 Episodicity and growth of the Cordilleran Median Batholith

It has long been noted (e.g. Mortimer et al., 1999b; Price et al., 2006; Tulloch and Kimbrough, 2003) that the axis of Mesozoic continental magmatism, as defined by pluton crystallization ages, migrated west in southern South Island from the Triassic to Early Cretaceous. As more plutons have been dated it has been possible to go from a very

provisional picture of magmatic pulses and gaps (e.g. see Figure 4 in Mortimer et al., 1999b) to more a complete picture of magma flux rates (e.g. see Figure 3 in Ringwood et al., 2021). The establishment of the Late Permian Longwood Suite (McCoy-West et al. 2014; this paper) defines even longer spatial and temporal baselines, and wider isotopic and geochemical variations in this across-strike migration of continental arc volcanism than has previously been recognized in New Zealand (Fig. 8; cf. Chapman et al., 2017) .

Plutons of the 350-342 Ma I-type Tobin Suite are interpreted to represent continental arc magmatism (Tulloch et al., 2009). As yet no clearly subduction-related plutons in New Zealand's Median or other batholiths have been dated in the interval 342-261 Ma. The presence of scattered plutons of the anorogenic A-type Foulwind Suite (Fig. 8b; c. 330-305 Ma) reaffirms that for c. 80 Ma. there was seemingly no magmatic record of subduction under the Zealandia part of the Gondwana supercontinent margin. The re-initiation of isotopically primitive Longwood Suite continental arc magmatism at c. 261 Ma was thus an episode of major tectonomagmatic change. The isotopically primitive nature of the Longwood Suite (Fig. 5) fits with its easterly position (Fig. 8a) in as much as deeper domains of radiogenic crust would be thin or absent. The slightly more isotopically evolved (yet younger) Darran Suite, lying to the west might have interacted with a different and distinct lower crustal block within its source region (cf. Chapman et al., 2017).

With the eastward growth of the Eastern Province accretionary wedge in the Mesozoic, a westward migration of subduction-related co-eval magmatism (Longwood to Darran to Separation Point suites; Fig. 8a) had to have been accompanied by a long-term shallowing of the dip of the subducting slab. The role of deep crustal domains in the overriding Gondwana plate as controls on magma chemistry has started to be revealed by recent studies (e.g. Schwartz et al., 2021; Turnbull et al., 2021) and the Longwood Suite will be a useful end-member to incorporate in future interpretations.

6.0 Conclusions

The Late Permian to Middle Triassic Longwood Suite, the easternmost plutonic suite in the Median Batholith, is isotopically more primitive and chemically distinct from both the older and younger suites of the Median Batholith. Our new geochronological and geochemical study of the coeval plutons of leucotonalite (trondhjemites) that intrude layered mafic-ultramafic plutonic complexes of the Longwood Suite confirms and extends earlier interpretations by McCoy-West et al. (2014):

- (1) We define new geochemical criteria to characterize Longwood Suite granitoids. Longwood Suite granitoids are I-type and sodic ($K/Na < 0.4$), with distinctive low Rb and Nb/Ta and notably flat rare earth element patterns ($La/Yb_N < 10$). They also have uniquely unradiogenic $^{87}Sr/^{86}Sr_{(t)}$ (0.7029 to 0.7032) and radiogenic $\epsilon^{143}Nd_{(t)}$ (+6.3 to +8.2), which clearly distinguishes them from the I-type Darran Suite plutons that intrude them.
- (2) New U-Pb zircon crystallization ages of 258.5 ± 2.5 Ma, 256.0 ± 1.8 Ma, 247.8 ± 2.7 Ma and 243.2 ± 2.4 Ma obtained from plutons on Ruapuke Island, and a gabbroic dike at Bluff, supplement previous geochronology. These ages confirm the restricted time range (c. 261-243 Ma) of the Longwood Suite and expand its areal extent south into Foveaux Strait.
- (3) Longwood Suite samples have highly variable stable Nd isotope compositions (-0.075 ‰ to $+0.158$ ‰; $\delta^{146}Nd = 233$ ppm) compared to previously analysed plutonic rocks ($\delta^{146}Nd = 44$ ppm), which are indistinguishable from bulk silicate Earth. A Pourakino Trondhjemite dike has the heaviest $\delta^{146}Nd$ observed globally at $+0.158$ ‰. This heavy composition requires light Nd isotopes to have been sequestered into REE-rich

accessory phases (e.g. monazite), which must have remained trapped in the parental magma chamber.

(4) Despite its primitive character based on onland exposure areas only, the Longwood Suite has a maximum areal magma addition rate of c. 11 km²/Ma, which is substantially less than the 27-67 km²/Ma and 105-375 km²/Ma of the Darran Suite and Separation Point Suite, respectively, when the magmatic arc was fully established.

(5) Prior to primitive Permian magmatism, the Gondwanan lithosphere is inferred to have been thin, as demonstrated by extension and basin development along this segment of the Gondwana margin. This is consistent with the geochemical characteristics of the Pourakino Trondhjemite (i.e. low La/Yb_(N) and Nb/Ta) which indicate generation by shallow melting (< 28 km) of an garnet-free amphibolitic residue. In this instance, calculations of crustal thickness using Sr/Y produce highly erroneous results.

(6) Collectively, these unique petrologic and geochemical features point to a special tectonomagmatic setting for petrogenesis and emplacement of the Longwood Suite, effectively the re-initiation of a subduction-related continental arc. We suggest a model for Longwood Suite magmagenesis involving a phase of renewed Gondwana margin tectonic convergence (the Hunter-Bowen orogeny). This convergence led to the tectonic underplating of Permian intra-oceanic island arc crust and mantle under the Gondwana margin. In turn, melting of the underplated arc crust and mantle generated the isotopically primitive Longwood Suite trondhjemite and gabbro plutons.

Collision and underplating of mafic oceanic terranes, including large igneous provinces, with a continental margin is not uncommon in the geological record. Largely bimodal plutonism may be one consequence of such events.

658

659 **ACKNOWLEDGEMENTS**

660 We thank the University of Otago, Department of Geology for permission to use Ruapuke
661 Island material from its rock collection. Geoff Nowell, Chris Ottley and Peter Holden are
662 thanked for analytical assistance. Ben Durrant, John Simes and Belinda Smith-Lyttle are
663 acknowledged for thin section and mineral separation work. We thank Hamish Campbell and
664 Gideon Rosenbaum for discussions about Permian Gondwana, and Priyadarshi Chowdhury
665 for discussion of trondhjemite genesis. An earlier version of the manuscript was improved by
666 comments from Matt Sagar. Josh Schwartz and an anonymous referee are thanked for
667 thought-provoking journal reviews. NM's contribution was supported by core funding to
668 GNS Science from the New Zealand Ministry of Business, Innovation and Employment
669 contract C05X1103. This project was also funded by NERC grant NE/N003926/1 and ARC
670 grant FL160100168.

671

672 **AUTHOR CONTRIBUTIONS**

673 **AMW:** Conceptualization, Investigation, Visualization, Formal analysis, Methodology
674 Writing - Original Draft; **NM:** Conceptualization, Visualization, Writing- Original Draft;
675 **KB:** Resources, Funding acquisition; **TI:** Resources, Validation; **PC:** Writing- Reviewing
676 and Editing, Funding acquisition

677

678

679

680

681

682 **References**

- 683 Adams, C.J., Barley, M.E., Maas, R., Doyle, M.G., 2002. Provenance of Permian-Triassic volcanoclastic
684 sedimentary terranes in New Zealand: Evidence from their radiogenic isotope characteristics and detrital
685 mineral age patterns. *New Zealand J. Geol. Geophys.* 45, 221-242.
- 686 Adams, C.J., Pankhurst, R.J., Maas, R., Millar, I.L., 2005. Nd and Sr isotopic signatures of metasedimentary
687 rocks around the South Pacific margin and implications for their provenance. *Geol. Soc. Spec. Publ.* 246, 113-
688 141.
- 689 Allibone, A.H., Cox, S.C., Graham, I.J., Smellie, R.W., Johnstone, R.D., Ellery, S.G., Palmer, K., 1993.
690 Granitoids of the Dry Valleys area, southern Victoria Land, Antarctica: Plutons, field relationships, and isotopic
691 dating. *New Zealand J. Geol. Geophys.* 36, 281-297.
- 692 Allibone, A.H., Jongens, R., Scott, J.M., Tulloch, A.J., Turnbull, I.M., Cooper, A.F., Powell, N.G., Ladley,
693 E.B., King, R.P., Rattenbury, M.S., 2009. Plutonic rocks of the Median Batholith in eastern and central
694 Fiordland, New Zealand: Field relations, geochemistry, correlation, and nomenclature. *New Zealand J. Geol.*
695 *Geophys.* 52, 101-148.
- 696 Allibone, A.H., Tulloch, A.J., 2004. Geology of the plutonic basement rocks of Stewart Island, New Zealand *J.*
697 *Geol. Geophys.* 47, 233-256.
- 698 Allibone, A.H., Turnbull, I.M., Tulloch, A.J., Cooper, A.F., 2007. Plutonic rocks of the Median Batholith in
699 southwest Fiordland, New Zealand: Field relations, geochemistry, and correlation. *New Zealand J. Geol.*
700 *Geophys.* 50, 283-314.
- 701 Ashley, P., Craw, D., MacKenzie, D., Rombouts, M., Reay, A., 2012. Mafic and ultramafic rocks, and platinum
702 mineralisation potential, in the Longwood Range, Southland, New Zealand. *New Zealand J. Geol. Geophys.* 55,
703 3-19.
- 704 Barker, F., Arth, J.G., 1976. Generation of trondhjemitic-tonalitic liquids and Archean bimodal trondhjemite-
705 basalt suites. *Geology* 4, 596-600.
- 706 Black, L.P., Kamo, S.L., Allen, C.M., Aleinikoff, J.N., Davis, D.W., Korsch, R.J., Foudoulis, C., 2003.
707 TEMORA 1: A new zircon standard for Phanerozoic U-Pb geochronology. *Chem. Geol.* 200, 155-170.
- 708 Bryant, C.J., Arculus, R.J., Chappell, B.W., 1997. Clarence River Supersuite: 250 Ma Cordilleran Tonalitic I-
709 type Intrusions in Eastern Australia. *J. Petrol.* 38, 975-1001.
- 710 Buriticá, L.F., Schwartz, J.J., Klepeis, K.A., Miranda, E.A., Tulloch, A.J., Coble, M.A., Kylander-Clark,
711 A.R.C., 2019. Temporal and spatial variations in magmatism and transpression in a Cretaceous arc, Median
712 Batholith, Fiordland, New Zealand. *Lithosphere* 11, 652-682.
- 713 Campbell, H.J., 2019. Chapter 3: Biostratigraphic age review of New Zealand's Permian–Triassic central
714 terranes. *Geol. Soc. London Mem.* 49, 31-41.

- 715 Campbell, M.J., Rosenbaum, G., Allen, C.M., Spandler, C., 2020. Continental crustal growth processes revealed
716 by detrital zircon petrochronology: Insights from Zealandia. *J. Geophys. Res.* 125, e2019JB019075.
- 717 Cawood, P., Leitch, E., Merle, R.E., Nemchin, A., 2011a. Orogenesis without collision: Stabilizing the Terra
718 Australis accretionary orogen, eastern Australia. *Geol. Soc. Am. Bull.* 123, 2240-2255.
- 719 Cawood, P.A., 1984. The development of the SW Pacific margin of Gondwana: correlations between the
720 Rangitata and New England orogens. *Tectonics* 3, 539-553.
- 721 Cawood, P.A., 2005. Terra Australis Orogen: Rodinia breakup and development of the Pacific and Iapetus
722 margins of Gondwana during the Neoproterozoic and Paleozoic. *Earth Sci. Rev.* 69, 249-279.
- 723 Cawood, P.A., Pisarevsky, S.A., Leitch, E.C., 2011b. Unraveling the New England orocline, east Gondwana
724 accretionary margin. *Tectonics* 30, TC5002, doi:10.1029/2011TC002864.
- 725 Challis, G.A., Lauder, W.R., 1977. The pre-Tertiary geology of the Longwood Range. Department of Scientific
726 and Industrial Research, Wellington, New Zealand, pp. New Zealand Geological Survey Miscellaneous Series,
727 Map 11 11:50,000.
- 728 Chapman, J.B., Ducea, M.N., DeCelles, P.G., Profeta, L., 2015. Tracking changes in crustal thickness during
729 orogenic evolution with Sr/Y: An example from the North American Cordillera. *Geology* 43, 919-922.
- 730 Chapman, J.B., Ducea, M.N., Kapp, P., Gehrels, G.E., DeCelles, P.G., 2017. Spatial and temporal radiogenic
731 isotopic trends of magmatism in Cordilleran orogens. *Gondwana Res.* 48, 189-204.
- 732 Charlier, B.L.A., Ginibre, C., Morgan, D., Nowell, G.M., Pearson, D.G., Davidson, J.P., Ottley, C.J., 2006.
733 Methods for the microsampling and high-precision analysis of strontium and rubidium isotopes at single crystal
734 scale for petrological and geochronological applications. *Chem. Geol.* 232, 114-133.
- 735 Cowden, A., Ruddock, R., Reay, A., Nicolson, P., Waterman, P., Banks, M.J., 1990. Platinum mineralisation
736 potential of the Longwood Igneous Complex, New Zealand. *Mineral. Petrol.* 42, 181-195.
- 737 Dauphas, N., Craddock, P.R., Asimow, P.D., Bennett, V.C., Nutman, A.P., Ohnenstetter, D., 2009. Iron isotopes
738 may reveal the redox conditions of mantle melting from Archean to Present. *Earth Planet. Sci. Lett.* 288, 255-
739 267.
- 740 Decker, M., Schwartz, J.J., Stowell, H.H., Klepeis, K.A., Tulloch, A.J., Kitajima, K., Valley, J.W., Kylander-
741 Clark, A.R.C., 2017. Slab-Triggered Arc Flare-up in the Cretaceous Median Batholith and the Growth of Lower
742 Arc Crust, Fiordland, New Zealand. *J. Petrol.* 58, 1145-1171.
- 743 Devereux, I., McDougall, I., Watters, W.A., 1968. Potassium-Argon mineral dates on intrusive rocks from the
744 Foveaux Strait area. *New Zealand J. Geol. Geophys.* 11, 1230-1234.
- 745 Donchak, P.J.T., Purdy, D.J., Withnall, I.W., Blake, P.R., Jell, P.A., 2013. New England Orogen, In: Jell, P.A.
746 (Ed.), *Geology of Queensland*. Geological Survey of Queensland, Australia, pp. 305-472.

- 747 Drummond, M.S., Defant, M.J., 1990. A model for Trondhjemite-Tonalite-Dacite genesis and crustal growth
748 via slab melting: Archean to modern comparisons. *J. Geophys. Res.* 95, 21503-21521.
- 749 Exley, R.A., 1980. Microprobe studies of REE-rich accessory minerals: Implications for Skye granite
750 petrogenesis and REE mobility in hydrothermal systems. *Earth Planet. Sci. Lett.* 48, 97-110.
- 751 Frost, C.D., Coombs, D.S., 1989. Nd isotope character of New Zealand sediments: Implications for terrane
752 concepts and crustal evolution. *Amer. J. Sci.* 289, 744-770.
- 753 Gromet, P., Silver, L.T., 1987. REE Variations Across the Peninsular Ranges Batholith: Implications for
754 Batholithic Petrogenesis and Crustal Growth in Magmatic Arcs. *J. Petrol.* 28, 75-125.
- 755 Hensel, H.D., McCulloch, M.T., Chappell, B.W., 1985. The New England Batholith: constraints on its
756 derivation from Nd and Sr isotopic studies of granitoids and country rocks. *Geochim. Cosmochim. Acta* 49,
757 369-384.
- 758 Hoskin, P.W.O., 2000. Patterns of chaos: Fractal statistics and the oscillatory chemistry of zircon. *Geochim.*
759 *Cosmochim. Acta* 64, 1905-1923.
- 760 Houghton, B.F., 1981. Lithostratigraphy of the Takitimu Group, central Takitimu Mountains, western
761 Southland, New Zealand. *New Zealand J. Geol. Geophys.* 24, 333-348.
- 762 Houghton, B.F., 1985. Petrology of the calcalkaline lavas of the Permian Takitimu Group, southern New
763 Zealand. *New Zealand J. Geol. Geophys.* 28, 649-665.
- 764 Houghton, B.F., Landis, C.A., 1989. Sedimentation and volcanism in a Permian arc-related basin, southern New
765 Zealand. *Bull. Volcanol.* 51, 433-450.
- 766 Ireland, T.R., Williams, I.S., 2003. Considerations in Zircon Geochronology by SIMS. *Rev. Mineral. Geochem.*
767 53, 215-241.
- 768 Jacobsen, S.B., Wasserburg, G.J., 1984. Sm-Nd isotopic evolution of chondrites and achondrites, II. *Earth*
769 *Planet. Sci. Lett.* 67, 137-150.
- 770 Jessop, K., Daczko, N.R., Piazzolo, S., 2019. Tectonic cycles of the New England Orogen, eastern Australia: A
771 Review. *Aust. J. Earth Sci.* 66, 459-496.
- 772 Kemp, A.I.S., Hawkesworth, C.J., Collins, W.J., Gray, C.M., Blevin, P.L., 2009. Isotopic evidence for rapid
773 continental growth in an extensional accretionary orogen: The Tasmanides, eastern Australia. *Earth Planet. Sci.*
774 *Lett.* 284, 455-466.
- 775 Kimbrough, D.L., Mattinson, J.M., Coombs, D.S., Landis, C.A., Johnston, M.R., 1992. Uranium-lead ages from
776 the Dun Mountain ophiolite belt and Brook Street terrane, South Island, New Zealand. *Geol. Soc. Am. Bull.*
777 104, 429-443.

- Kimbrough, D.L., Tulloch, A.J., Coombs, D.S., Landis, C.A., Johnston, M.R., Mattinson, J.M., 1994. Uranium-lead zircon ages from the Median Tectonic Zone, New Zealand. *New Zealand J. Geol. Geophys.* 37, 393-419.
- Landis, C., Coombs, D., 1967. Metamorphic belts and orogenesis in southern New Zealand. *Tectonophysics* 4, 501-518.
- Landis, C.A., Campbell, H.J., Aslund, T., Cawood, P.A., Douglas, A., Kimbrough, D.L., Pillai, D.D.L., Raine, J.I., Willsman, A., 1999. Permian-Jurassic strata at Productus Creek, Southland, New Zealand: Implications for terrane dynamics of the eastern Gondwanaland margin. *New Zealand J. Geol. Geophys.* 42, 255-278.
- Li, L., Xiong, X.L., Liu, X.C., 2017. Nb/Ta Fractionation by Amphibole in Hydrous Basaltic Systems: Implications for Arc Magma Evolution and Continental Crust Formation. *J. Petrol.* 58, 3-28.
- Li, P., Rosenbaum, G., Yang, J.-H., Hoy, D., 2015. Australian-derived detrital zircons in the Permian-Triassic Gympie terrane (eastern Australia): Evidence for an autochthonous origin. *Tectonics* 34, 858-874.
- Liu, J., Scott, J.M., Martin, C.E., Pearson, D.G., 2015. The longevity of Archean mantle residues in the convecting upper mantle and their role in young continent formation. *Earth Planet. Sci. Lett.* 424, 109-118.
- Mantle, G., Collins, W., 2008. Quantifying crustal thickness variations in evolving orogens: Correlation between arc basalt composition and Moho depth. *Geology* 36, 87-90.
- Matthews, K.J., Maloney, K.T., Zahirovic, S., Williams, S.E., Seton, M., Mueller, R.D., 2016. Global plate boundary evolution and kinematics since the late Paleozoic. *Glob. Planet. Change* 146, 226-250.
- McCoy-West, A.J., Bennett, V.C., Amelin, Y., 2016. Rapid Cenozoic ingrowth of isotopic signatures simulating “HIMU” in ancient lithospheric mantle: Distinguishing source from process. *Geochim. Cosmochim. Acta* 187, 79-101.
- McCoy-West, A.J., Bennett, V.C., Puchtel, I.S., Walker, R.J., 2013. Extreme persistence of cratonic lithosphere in the Southwest Pacific: Paleoproterozoic Os isotopic signatures of Zealandia. *Geology* 41, 231-234.
- McCoy-West, A.J., Burton, K.W., Millet, M.-A., Cawood, P.A., 2021. The chondritic neodymium stable isotope composition of the Earth inferred from mid-ocean ridge, ocean island and arc basalts. *Geochim. Cosmochim. Acta* 293, 575-597.
- McCoy-West, A.J., Chowdhury, P., Burton, K.W., Sossi, P., Nowell, G.M., Fitton, J.G., Kerr, A.C., Cawood, P.A., Williams, H.M., 2019. Extensive crustal extraction in Earth’s early history inferred from molybdenum isotopes. *Nat. Geosci.* 12, 946-951.
- McCoy-West, A.J., Millet, M.-A., Burton, K.W., 2017. The neodymium stable isotope composition of the silicate Earth and chondrites. *Earth Planet. Sci. Lett.* 480, 121-132.
- McCoy-West, A.J., Millet, M.-A., Burton, K.W., 2020a. The neodymium stable isotope composition of the oceanic crust: Reconciling the mismatch between erupted mid-ocean ridge basalts and lower crustal gabbros. *Front. Earth Sci.* 8.

- 811 McCoy-West, A.J., Millet, M.-A., Nowell, G.M., Nebel, O., Burton, K.W., 2020b. Simultaneous measurement
812 of neodymium stable and radiogenic isotopes from a single aliquot using a double spike. *J. Anal. At. Spectrom.*
813 35, 388-402.
- 814 McCoy-West, A.J., Mortimer, N., Ireland, T.R., 2014. U–Pb geochronology of Permian plutonic rocks,
815 Longwood Range, New Zealand: implications for Median Batholith–Brook Street Terrane relations. *New*
816 *Zealand J. Geol. Geophys.* 57, 65-85.
- 817 Milan, L.A., Daczko, N.R., Clarke, G.L., 2017. Cordillera Zealandia: A Mesozoic arc flare-up on the palaeo-
818 Pacific Gondwana Margin. *Sci. Rep.* 7, 261.
- 819 Mortimer, N., 2004. New Zealand's geological foundations. *Gondwana Res.* 7, 261-272.
- 820 Mortimer, N., 2014. The oroclinal bend in the South Island, New Zealand. *J. Struct. Geol.* 64, 32-38.
- 821 Mortimer, N., Campbell, H.J., 2014. Zealandia: Our continent revealed. Penguin Books, New Zealand.
- 822 Mortimer, N., Campbell, H.J., Tulloch, A.J., King, P.R., Stagpoole, V.M., Wood, R.A., Rattenbury, M.S.,
823 Sutherland, R., Adams, C.J., Collot, J.Y., Seton, M., 2017. Zealandia: Earth's hidden continent. *GSA Today* 27,
824 27-35.
- 825 Mortimer, N., Caratori-Tontini, F., Martin, C.E., 2016. Revised three-dimensional geometry of the platiniferous
826 Hekeia Gabbro, Longwood Range, Southland, Australasian Institute of Mining and Metallurgy (AUSIMM)
827 Monographs, pp. 487-492.
- 828 Mortimer, N., Craw, D., Ashley, P., Christie, A., Mackenzie, D., 2011. Potentially platiniferous mafic bodies on
829 the Gondwana margin, New Zealand and Australia, AUSIMM New Zealand Branch Conference Proceedings,
830 44, pp. 327-336.
- 831 Mortimer, N., Gans, P., Calvert, A., Walker, N., 1999a. Geology and thermochronometry of the east edge of the
832 Median Batholith (Median Tectonic Zone): A new perspective on Permian to Cretaceous crustal growth of New
833 Zealand. *Isl. Arc* 8, 404-425.
- 834 Mortimer, N., Herzer, R.H., Gans, P.B., Parkinson, D.L., Seward, D., 1998. Basement geology from Three
835 Kings Ridge to West Norfolk Ridge, southwest Pacific Ocean: Evidence from petrology, geochemistry and
836 isotopic dating of dredge samples. *Mar. Geol.* 148, 135-162.
- 837 Mortimer, N., Rattenbury, M.S., King, P.R., Bland, K.J., Barrell, D.J.A., Bache, F., Begg, J.G., Campbell, H.J.,
838 Cox, S.C., Crampton, J.S., Edbrooke, S.W., Forsyth, P.J., Johnston, M.R., Jongens, R., Lee, J.M., Leonard,
839 G.S., Raine, J.I., Skinner, D.N.B., Timm, C., Townsend, D.B., Tulloch, A.J., Turnbull, I.M., Turnbull, R.E.,
840 2014. High-level stratigraphic scheme for New Zealand rocks. *New Zealand J. Geol. Geophys.* 57, 402-419.
- 841 Mortimer, N., Tulloch, A.J., Spark, R.N., Walker, N.W., Ladley, E., Allibone, A., Kimbrough, D.L., 1999b.
842 Overview of the Median Batholith, New Zealand: A new interpretation of the geology of the Median Tectonic
843 Zone and adjacent rocks. *J. Afr. Earth Sci.* 29, 257-268.

- 844 Mossman, D.J., 1973. Geology of the Greenhills Ultramafic Complex, Bluff Peninsula, Southland, New
845 Zealand. *Geol. Soc. Am. Bull.* 84, 39-62.
- 846 Moyen, J.-F., 2011. The composite Archaean grey gneisses: Petrological significance, and evidence for a non-
847 unique tectonic setting for Archaean crustal growth. *Lithos* 123, 21-36.
- 848 Muir, R.J., Ireland, T.R., Weaver, S.D., Bradshaw, J.D., 1994. Ion microprobe U-Pb zircon geochronology of
849 granitic magmatism in the Western Province of the South Island, New Zealand. *Chem. Geol.* 113, 171-189.
- 850 Muir, R.J., Ireland, T.R., Weaver, S.D., Bradshaw, J.D., 1996a. Ion microprobe dating of Paleozoic granitoids:
851 Devonian magmatism in New Zealand and correlations with Australia and Antarctica. *Chem. Geol.* 127, 191-
852 210.
- 853 Muir, R.J., Ireland, T.R., Weaver, S.D., Bradshaw, J.D., Evans, J.A., Eby, G.N., Shelley, D., 1998.
854 Geochronology and geochemistry of a Mesozoic magmatic arc system, Fiordland, New Zealand. *J. Geol. Soc.*
855 London 155, 1037-1053.
- 856 Muir, R.J., Ireland, T.R., Weaver, S.D., Bradshaw, J.D., Waight, T.E., Jongens, R., Eby, G.N., 1997. SHRIMP
857 U-Pb geochronology of Cretaceous magmatism in northwest Nelson-Westland, South Island, New Zealand.
858 New Zealand J. Geol. Geophys. 40, 453-463.
- 859 Muir, R.J., Weaver, S.D., Bradshaw, J.D., Eby, G.N., Evans, J.A., 1995. The Cretaceous Separation Point
860 batholith, New Zealand: granitoid magmas formed by melting of mafic lithosphere. *J. Geol. Soc. London* 152,
861 689.
- 862 Muir, R.J., Weaver, S.D., Bradshaw, J.D., Eby, G.N., Evans, J.A., Ireland, T.R., 1996b. Geochemistry of the
863 Karamea Batholith, New Zealand and comparisons with the Lachlan Fold Belt granites of SE Australia. *Lithos*
864 39, 1-20.
- 865 Nebel, O., Münker, C., Nebel-Jacobsen, Y.J., Kleine, T., Mezger, K., Mortimer, N., 2007. Hf-Nd-Pb isotope
866 evidence from Permian arc rocks for the long-term presence of the Indian-Pacific mantle boundary in the SW
867 Pacific. *Earth Planet. Sci. Lett.* 254, 377-392.
- 868 Nelson, D., Cottle, J., 2017. Long- term geochemical and geodynamic segmentation of the paleo- Pacific
869 margin of Gondwana: Insight from the Antarctic and adjacent sectors. *Tectonics* 36, 3229-3247.
- 870 Ottley, C., Pearson, G., Irvine, G.J., 2003. A Routine Method for the Dissolution of Geological Samples for the
871 Analysis of REE and Trace Elements via ICP-MS. *Plasma Source Mass Spectrometry: Applications and*
872 *Emerging Technologies.* 221-230.
- 873 Palme, H., O'Neill, H.S.C., 2014. 3.1 - Cosmochemical estimates of mantle composition, In: Holland, H.D.,
874 Turekian, K.K. (Eds.), *Treatise on Geochemistry (Second Edition)*. Elsevier, Oxford, pp. 1-39.

- 875 Paterson, S.R., Okaya, D., Memeti, V., Economos, R., Miller, R.B., 2011. Magma addition and flux calculations
876 of incrementally constructed magma chambers in continental margin arcs: Combined field, geochronologic, and
877 thermal modeling studies. *Geosphere* 7, 1439-1468.
- 878 Pearce, J.A., Harris, N.B.W., Tindle, A.G., 1984. Trace Element Discrimination Diagrams for the Tectonic
879 Interpretation of Granitic Rocks. *J. Petrol.* 25, 956-983.
- 880 Pickett, D.A., Wasserburg, G.J., 1989. Neodymium and strontium isotopic characteristics of New Zealand
881 granitoids and related rocks. *Contrib. Mineral. Petrol.* 103, 131-142.
- 882 Price, R., Spandler, C., Arculus, R., Reay, A., 2011. The Longwood Igneous Complex, Southland, New
883 Zealand: A Permo-Jurassic, intra-oceanic, subduction-related, I-type batholithic complex. *Lithos* 126, 1-21.
- 884 Price, R.C., Ireland, T.R., Maas, R., Arculus, R.J., 2006. SHRIMP ion probe zircon geochronology and Sr and
885 Nd isotope geochemistry for southern Longwood Range and Bluff Peninsula intrusive rocks of Southland, New
886 Zealand. *New Zealand J. Geol. Geophys.* 49, 291-303.
- 887 Profeta, L., Ducea, M.N., Chapman, J.B., Paterson, S.R., Gonzales, S.M.H., Kirsch, M., Petrescu, L., DeCelles,
888 P.G., 2015. Quantifying crustal thickness over time in magmatic arcs. *Sci. Rep.* 5, 17786.
- 889 Ramezani, J., Tulloch, A.J., 2006. U-Pb geochronology of plutons from SW Fiordland, GNS Technical File
890 Report QM417/594 [BIB ID 168878]. GNS Science, Lower Hutt, p. 26.
- 891 Ramezani, J., Tulloch, A.J., 2009. TIMS U-Pb geochronology of dioritic-granitic rocks, Fiordland, GNS
892 Technical File Report QM417/594 [BIB ID 232315]. GNS Science, Lower Hutt, p. 37.
- 893 Rapp, R.P., Shimizu, N., Norman, M.D., 2003. Growth of early continental crust by partial melting of eclogite.
894 *Nature* 425, 605-609.
- 895 Rapp, R.P., Watson, E.B., Miller, C.F., 1991. Partial melting of amphibolite/eclogite and the origin of Archean
896 trondhjemites and tonalites. *Precambrian Res.* 51, 1-25.
- 897 Rattenbury, M.S., Cooper, R.A., Johnston, M.R., 1998. Geology of the Nelson area, In: Rattenbury, M.S.,
898 Cooper, R.A., Johnston, M.R. (Eds.), 1:250,000 Geological Map 9. 1 sheet + 67p. Institute of Geological and
899 Nuclear Sciences, Lower Hutt, New Zealand.
- 900 Ringwood, M.F., Schwartz, J.J., Turnbull, R.E., Tulloch, A.J., 2021. Phanerozoic record of mantle-dominated
901 arc magmatic surges in the Zealandia Cordillera. *Geology* in press, doi.org/10.1130/G48916.48911.
- 902 Robertson, A.H.F., Palamakumbura, R., 2019. Chapter 4 Geological development and regional significance of
903 an oceanic magmatic arc and its sedimentary cover: Permian Brook Street Terrane, South Island, New Zealand.
904 *Geol. Soc. Lond. Mem.* 49, 43-73.
- 905 Rosenbaum, G., 2018. The Tasmanides: Phanerozoic tectonic evolution of eastern Australia. *Annu. Rev. Earth
906 Planet. Sci.* 46, 291-325.

- 907 Rushmer, T., 1991. Partial melting of two amphibolites: contrasting experimental results under fluid-absent
908 conditions. *Contrib. Mineral. Petrol.* 107, 41-59.
- 909 Savage, P.S., Georg, R.B., Williams, H.M., Burton, K.W., Halliday, A.N., 2011. Silicon isotope fractionation
910 during magmatic differentiation. *Geochim. Cosmochim. Acta* 75, 6124-6139.
- 911 Schwartz, J.J., Andico, S., Turnbull, R., Klepeis, K.A., Tulloch, A., Kitajima, K., Valley, J.W., 2021. Stable and
912 Transient Isotopic Trends in the Crustal Evolution of Zealandia Cordillera. *Am. Min.* in press, doi:10.2138/am-
913 2021-7626.
- 914 Schwartz, J.J., Klepeis, K.A., Sadorski, J.F., Stowell, H.H., Tulloch, A.J., Coble, M.A., 2017. The tempo of
915 continental arc construction in the Mesozoic Median Batholith, Fiordland, New Zealand. *Lithosphere* 9, 343-
916 365.
- 917 Scott, J.M., Palin, J.M., 2008. LA-ICP-MS U-Pb zircon ages from Mesozoic plutonic rocks in eastern Fiordland,
918 New Zealand *J. Geol. Geophys.* 51, 105-113.
- 919 Service, H., 1937. An intrusion of norite and its accompanying contact metamorphism at Bluff, New Zealand.
920 *Transactions and Proceedings of the Royal Society of New Zealand* 67, 185-217.
- 921 Shaw, S., Flood, R., 1981. The New England Batholith, eastern Australia: geochemical variations in time and
922 space. *J. Geophys. Res.: Solid Earth* 86, 10530-10544.
- 923 Shaw, S.E., Flood, R.H., Pearson, N.J., 2011. The New England Batholith of eastern Australia: Evidence of
924 silicic magma mixing from zircon $^{176}\text{Hf}/^{177}\text{Hf}$ ratios. *Lithos* 126, 115-126.
- 925 Sivell, W., Rankin, P., 1983. Arc-tholeiite and ultramafic cumulate, Brook Street Volcanics, west D'Urville
926 Island, New Zealand. *New Zealand J. Geol. Geophys.* 26, 239-257.
- 927 Spandler, C., Arculus, R., Eggins, S., Mavrogenes, J., Price, R., Reay, A., 2003. Petrogenesis of the Greenhills
928 Complex, Southland, New Zealand: Magmatic differentiation and cumulate formation at the roots of a Permian
929 island-arc volcano. *Contrib. Mineral. Petrol.* 144, 703-721.
- 930 Spandler, C., Worden, K., Arculus, R., Eggins, S., 2005. Igneous rocks of the Brook Street Terrane, New
931 Zealand: Implications for Permian tectonics of eastern Gondwana and magma genesis in modern intra-oceanic
932 volcanic arcs. *New Zealand J. Geol. Geophys.* 48, 167 - 183.
- 933 Spandler, C.J., Eggins, S.M., Arculus, R.J., Mavrogenes, J.A., 2000. Using melt inclusions to determine parent-
934 magma compositions of layered intrusions: Application to the Greenhills Complex (New Zealand), a platinum
935 group minerals-bearing, island-arc intrusion. *Geology* 28, 991-994.
- 936 Steiger, R.H., Jäger, E., 1977. Subcommittee on geochronology: Convention on the use of decay constants in
937 geo- and cosmochemistry. *Earth Planet. Sci. Lett.* 36, 359-362.
- 938 Talusani, R.V.R., Sivell, W.J., Ashley, P.M., 2005. Mineral chemistry, petrogenesis, and tectonic setting of the
939 Wateranga layered intrusion, southeast Queensland, Australia. *Can. J. Earth Sci.* 42, 1967-1985.

- 940 Tate, M.C., Norman, M.D., Johnson, S.E., Fanning, C.M., Anderson, J.L., 1999. Generation of Tonalite and
941 Trondhjemite by Subvolcanic Fractionation and Partial Melting in the Zarza Intrusive Complex, Western
942 Peninsular Ranges Batholith, Northwestern Mexico. *J. Petrol.* 40, 983-1010.
- 943 Tera, F., Wasserburg, G.J., 1972. U-Th-Pb systematics in three Apollo 14 basalts and the problem of initial Pb
944 in lunar rocks. *Earth Planet. Sci. Lett.* 14, 281-304.
- 945 Thomson Aviation, 2020. Southern Mosaic, South Island, New Zealand. Data processing report for airborne
946 multi-survey grid. Mineral Report MR5729. New Zealand Petroleum and Minerals, Ministry of Business
947 Innovation and Employment.
- 948 Tiepolo, M., Bottazzi, P., Foley, S.F., Oberti, R., Vannucci, R., Zanetti, A., 2001. Fractionation of Nb and Ta
949 from Zr and Hf at Mantle Depths: The role of Titanian Pargasite and Kaersutite. *J. Petrol.* 42, 221-232.
- 950 Tulloch, A.J., 2001. Sr-Nd isotopic test for Brook Street affinity of rocks in NW Stewart Island and Ruapuke
951 Island, GNS Technical File Report D48/571 [BIB ID 152998]. GNS Science, Lower Hutt, p. 4.
- 952 Tulloch, A.J., Kimbrough, D.L., 2003. Paired plutonic belts in convergent margins and the development of high
953 Sr/Y magmatism: Peninsular Ranges batholith of Baja-California and Median batholith of New Zealand, In:
954 Johnson, S.E., Paterson, S.R., Fletcher, J.M., Girty, G.H., Kimbrough, D.L., Martín-Barajas, A. (Eds.), *Tectonic
955 evolution of northwestern México and the southwestern USA*. *Geol. Soc. Am. Spec. Pap.* 374, Boulder,
956 Colorado, pp. 275-295.
- 957 Tulloch, A.J., Kimbrough, D.L., Landis, C.A., Mortimer, N., Johnston, M.R., 1999. Relationships between the
958 Brook Street Terrane and Median Tectonic Zone (Median Batholith): Evidence from Jurassic conglomerates.
959 *New Zealand J. Geol. Geophys.* 42, 279-293.
- 960 Tulloch, A.J., Ramezani, J., Kimbrough, D.L., Faure, K., Allibone, A.H., 2009. U-Pb geochronology of mid-
961 Paleozoic plutonism in western New Zealand: Implications for S-type granite generation and growth of the east
962 Gondwana margin. *GSA Bull.* 121, 1236-1261.
- 963 Turnbull, I.M., Allibone, A.H., 2003. *Geology of the Murihiku area*. Institute of Geological and Nuclear
964 Sciences, Lower Hutt, New Zealand, pp. 1:250,000 Geological Map 220. 251 sheet + 274p.
- 965 Turnbull, R., Weaver, S., Tulloch, A., Cole, J., Handler, M., Ireland, T., 2010. Field and geochemical
966 constraints on mafic-felsic interactions, and processes in high-level arc magma chambers: An example from the
967 Halfmoon Pluton, New Zealand. *J. Petrol.* 51, 1477-1505.
- 968 Turnbull, R.E., Schwartz, J.J., Fiorentini, M.L., Jongens, R., Evans, N.J., Ludwig, T., McDonald, B.J., Klepeis,
969 K.A., 2021. A hidden Rodinian lithospheric keel beneath Zealandia, Earth's newly recognized continent.
970 *Geology*.
- 971 Turnbull, R.E., Size, W.B., Tulloch, A.J., Christie, A.B., 2017. The ultramafic–intermediate Riwaka Complex,
972 New Zealand: summary of the petrology, geochemistry and related Ni–Cu–PGE mineralisation. *New Zealand J.
973 Geol. Geophys.* 60, 270-295.

- 974 Veevers, J., 2004. Gondwanaland from 650–500 Ma assembly through 320 Ma merger in Pangea to 185–100
1 975 Ma breakup: supercontinental tectonics via stratigraphy and radiometric dating. *Earth Sci. Rev.* 68, 1-132.
2
3
4 976 Waight, T.E., Weaver, S.D., Muir, R.J., 1998a. Mid-Cretaceous granitic magmatism during the transition from
5 977 subduction to extension in southern New Zealand: A chemical and tectonic synthesis. *Lithos* 45, 469-482.
6
7 978 Waight, T.E., Weaver, S.D., Muir, R.J., Maas, R., Eby, G.N., 1998b. The Hohonu Batholith of North Westland,
8 979 New Zealand: granitoid compositions controlled by source H₂O contents and generated during tectonic
9
10 980 transition. *Contrib. Mineral. Petrol.* 130, 225-239.
11
12 981 Watters, W.A., 1978. Diorite and associated intrusive and metamorphic rocks between Port William and
13
14 982 Paterson Inlet, Stewart Island, and on Ruapuke Island. *New Zealand J. Geol. Geophys.* 21, 423-442.
15
16 983 Webster, J.G., 1981. The geology of Ruapuke Island, Geology Department. University of Otago, Dunedin, New
17
18 984 Zealand, p. 149.
19
20 985 Williams, J.G., Harper, C.T., 1978. Age and status of the Mackay Intrusives in the Eglinton—upper Hollyford
21
22 986 area. *New Zealand J. Geol. Geophys.* 21, 733-742.
23
24 987 Wilson, M., 1989. *Igneous petrogenesis: A global tectonic approach*. Unwin Hyman, London, 466 pp.
25
26 988 Wolf, M.B., Wyllie, P.J., 1994. Dehydration-melting of amphibolite at 10 kbar: the effects of temperature and
27
28 989 time. *Contrib. Mineral. Petrol.* 115, 369-383.
29
30 990
31
32
33 991 _____
34
35
36
37
38
39
40
41
42
43
44
45
46
47
48
49
50
51
52
53
54
55
56
57
58
59
60
61
62
63
64
65

Figure captions

Figure 1: Geological map of the southern South Island of New Zealand, modified after Turnbull and Allibone (2003) and McCoy-West et al. (2014). The box in the inset shows the area of the larger map. Areas labelled A, B, C, D refer to maps shown in Figure 2. PGC = Productus Creek Group

Figure 2: Sample locations, ages, and Nd isotope compositions in the context of local geology. (a) Longwood Range (Mortimer et al., 2016). Zircon crystallization ages for the Hekeia Gabbro are from McCoy-West et al. (2014). (b) Bluff area (Turnbull and Allibone, 2003). (c) Ruapuke Island (Webster, 1981). Inferred crystallization age and Nd isotope composition of Darran Suite sample P32760 are taken from Devereux et al. (1968) and Tulloch (2001), respectively. (d) Riwaka area, northwest Nelson (Rattenbury et al., 1998).

Figure 3: Tera-Wasserburg U-Pb zircon concordia plots of SHRIMP analyses of plutonic rocks from the Longwood Suite. (a) Greenhills Intrusion, Bluff Intrusive Complex, Bluff Peninsula; (b-d) Ruapuke Island plutons. Error ellipses are 1 s.d. uncertainties. Both common-Pb corrected ^{206}Pb - ^{238}U weighted mean ages (bold) and concordia intercept ages are reported with 2 s.d. uncertainties. The dashed line connects the concordia intercept age with composition of common Pb ($^{207}\text{Pb}/^{206}\text{Pb} = 0.83$). Analyses excluded from mean calculations are plotted with white circles and error ellipses.

Figure 4: Rare earth element and multi-element whole rock patterns for igneous rocks from southern New Zealand, chondrite-normalized and primitive mantle-normalized, respectively (Palme and O'Neill, 2014). (a-b) Brook Street Terrane samples, comparative data is taken from Spandler et al. (2005). (c-d) Intrusive Longwood Suite samples from the South Island. Existing data for the Pourakino Trondhjemite (Nebel et al., 2007) and Hollyburn Intrusives, Darran Suite (Price et al., 2006). (e-f) Ruapuke Island Intrusives and the Riwaka Granite, northwest Nelson compared to Longwood Suite.

Figure 5: Age corrected $^{87}\text{Sr}/^{86}\text{Sr}$ and $\epsilon^{143}\text{Nd}$ of magmatic rocks from southern New Zealand. Plutonic rocks are age corrected to their crystallization ages (Longwoods Suite: 261-243 Ma; Darran Suite: 232-128 Ma; Separation Point Suite: 125-115 Ma), with the age of the Brook Street Terrane samples assumed to be 285 Ma. We regard the Nd isotopic composition as less vulnerable to secondary processes than Sr isotopic composition, and therefore more reliable for comparative purposes. Hollow symbols represent previously published data for the suites analysed here. Previous data sources are as follows: Separation Point Suite (Muir et al., 1998; Muir et al., 1995); Darran Suite (Mortimer et al., 1999a; Muir et al., 1998; Price et al., 2006; Tulloch, 2001; Turnbull et al., 2010); Longwood Suite (Mortimer et al., 1999a; Price et al., 2006; Tulloch et al., 1999); Brook Street Terrane (Adams et al., 2005).

Figure 6: Comparison of $\delta^{146}\text{Nd}$ in extrusive and plutonic rocks from the South Island of New Zealand with global magmatic rocks. Data points are plotted with the long-term reproducibility of $\delta^{146}\text{Nd}$ ($\pm 0.015\text{‰}$). The yellow shaded area represents the bulk silicate Earth (BSE) average ($\delta^{146}\text{Nd} = -0.024 \pm 0.031\text{‰}$ (2 s.d.); McCoy-West et al., 2021). The shaded fields for the Brook Street Terrane and Longwood Suite also reflect ± 2 s.d. from the mean. Box and whisker plots were generated using data from previous studies: plutonic rocks ($n = 5$; McCoy-West et al., 2017), ocean floor gabbros ($n = 7$; McCoy-West et al., 2020a); arc basalts ($n = 12$; McCoy-West et al., 2021), mid-ocean ridge basalts ($n = 39$; McCoy-West et al., 2021; McCoy-West et al., 2017, 2020a).

Figure 7: Variations in $\delta^{146}\text{Nd}$ in plutonic rocks from New Zealand and globally. Graphs of $\delta^{146}\text{Nd}$ versus SiO_2 (a), Mg\# (b), and P_2O_5 (c), respectively. Mg\# (Magnesium-number) = molar $\text{Mg}/[\text{Mg} + \text{Fe}^{2+}]$. The yellow shaded area represents the bulk silicate Earth (BSE) average (McCoy-West et al., 2021). The sample denoted by the cross (P32769) has an elevated P_2O_5 relative to the other Longwood Suite samples because it is a hornblende-rich mafic mineral separate, not a conventional whole rock powder. The heavier $\delta^{146}\text{Nd}$ compositions of P81173 and P82430 are attributed to the previous removal of monazite and apatite, respectively.

Figure 8: The Longwood Suite in the context of other Tuhua Intrusives suites in the southern South Island. (a) Map showing the approximate position of the Median Batholith magmatic axis at different times. The distribution of individually-dated Darran (triangle), Longwood (circle) and Foulwind (square) samples with U-Pb crystallization ages are shown. (b) Histogram with 5 Ma bins showing the clear age distinction between the Foulwind Suite ($n = 6$), Longwood Suite ($n = 13$) and the Darran Suite ($n = 48$) within the area of the shown map. Probability density plot was generated using the same dataset assuming a minimum error of 3 Ma. Data is sourced from (herein; Kimbrough et al., 1992; Kimbrough et al., 1994; McCoy-West et al., 2014; Muir et al., 1998; Price et al., 2006; Ramezani and Tulloch, 2006, 2009; Schwartz et al., 2021; Scott and Palin, 2008; Tulloch et al., 1999; Tulloch et al., 2009).

Figure 9: Temporal evolution of geochemical signatures in rocks of the Median Batholith from 380 to 100 Ma. (a) $\varepsilon^{143}\text{Nd}$ of all rocks independent of SiO_2 . Symbols and references for Nd isotope data are the same as Figure 6, with additional Paleozoic data from Muir et al. (1996a), Muir et al. (1998) and Tulloch et al. (2009). A box and whisker plot for previous published data from the Brook Street Terrane is shown. (b-d) To limit the effect of magmatic differentiation only granitoids with >64 wt % SiO_2 are shown for trace element ratios (i.e. gabbros have lots of plagioclase and thus elevated Sr/Y). Additional trace element data is from Muir et al. (1997), Allibone et al. (2007), Scott and Palin (2008), Allibone et al. (2009) and Price et al. (2011). (b) Lines with values represent the median Sr/Y values for the major suites under discussion. Two samples from the Longwood Suite (hollow symbols) are excluded due to their distinct high-K composition. (c) Chondrite normalized (Palme and O'Neill, 2014) La/Yb . (d) Primitive mantle $\text{Nb/Ta} = 13.8 \pm 1.4$ (Palme and O'Neill, 2014). The Longwood Suite has the distinctive high $\varepsilon^{143}\text{Nd}$ and low $\text{La/Yb}_{(\text{N})}$ and Nb/Ta , compared with other suites within the Median Batholith.

Figure 10: Distinction of the Longwood and Darran Suites based on geochemistry. (a) Graph $\varepsilon^{143}\text{Nd}_{(\text{t})}$ versus SiO_2 content. Nd isotope data is corrected to the crystallization age of each sample. Data sources are the same as Fig. 6 with additional data from Nebel et al. (2007) and Mortimer et al. (2016). Hollow symbols represent previously published data for the Longwood Suite. (b) $\text{La/Sm}_{(\text{N})}$ versus SiO_2 , comparative data is from Muir et al. (1998), Nebel et al. (2007) and Price et al. (2011). (c) K/Na versus SiO_2 for granitoids $\text{SiO}_2 > 64$ wt %, calculated using the same dataset presented in Fig. 5. (d) Granite discrimination diagram (granitoids only) Rb concentration versus $\text{Y} + \text{Nb}$ after Pearce et al. (1984). Longwood Suite magmas have significantly lower $\text{La/Sm}_{(\text{N})}$, K and Rb than the younger suites of the Median Batholith.

Figure 11: Schematic model for the generation of the bimodal Longwood Suite gabbros and trondhjemites. (a) Early Permian Gondwana supercontinent margin was mainly passive (no magmatism, see Figure 8b) with formation of parautochthonous mafic intra-oceanic island arc terranes (green). (b) Late Permian tectonic underplating and melting of accreted terranes to generate a new, isotopically primitive, continental arc (red). Reconstructions based on Matthews et al. (2016);

this model draws on elements from Li et al. (2015) and Robertson and Palamakumbura (2019). NEO = New England Orogen; HBO = Hunter-Bowen Orogen.

Table Captions

Table 1: Summary of SHRIMP U-Pb zircon data for intrusive rocks of the Longwood Suite.

See Supplementary Data, Table S1 for complete U-Th-Pb isotopic compositions of the analysed zircons, 3 zircons were excluded for suspected Pb-loss or inheritance. Uncertainty on the mean ages are 2 s.d. and include propagated errors from the Temora standards.

Table 2: Whole rock Rb-Sr, Sm-Nd and Nd stable isotope data

Uncertainties on measured values are 2 standard errors. $\delta^{146}\text{Nd}_{(\text{NORM})}$ values have been normalized to JNdi-1 = 0‰ and uncertainties have been propagated. Radiogenic isotope data for the Longwoods Suite is age corrected using absolute crystallization ages (herein; McCoy-West et al., 2014). \$ ages have been estimated using nearby samples from the same unit. *Assumed to be 285 Ma, samples represent the lowest stratigraphic portion of the Brook Street Terrane, which is early Permian (c. 296-275 Ma) in age based on biostratigraphy (Campbell, 2019). No direct age constraints exist for the Riwaka Granite but it is probably part of the Paringa Suite (364 Ma; Tulloch et al., 2009) which exist nearby, see supplementary material for further discussion. $\epsilon^{143}\text{Nd}$ was calculated based on measured compositions, with $\epsilon^{143}\text{Nd} = [({}^{143}\text{Nd}/{}^{144}\text{Nd}_{\text{Sample}}/{}^{143}\text{Nd}/{}^{144}\text{Nd}_{\text{CHUR}}) - 1] \times 10,000$; assuming ${}^{143}\text{Nd}/{}^{144}\text{Nd}_{\text{CHUR}} = 0.512638$ and ${}^{147}\text{Sm}/{}^{144}\text{Nd}_{\text{CHUR}} = 0.1967$ (Jacobsen and Wasserburg, 1984). ^Brook Street Terrane samples with ${}^{87}\text{Sr}/{}^{86}\text{Sr}(\text{t}) > 0.7035$ should be interpreted with caution due to potential cryptic seawater contamination. # represents a replicate digestion processed through the chemical separation procedure.

Table 3: Calculated time-averaged areal magma addition rates for the Longwood, Darran and Separation Point suites.

Information for Darran and Separation Point suites in Fiordland from Milan et al. (2017) who, like us, used a time-averaged approach to calculate addition rates. More detailed pluton-specific analysis of magmatic fluxes in Fiordland can be found in Schwartz et al. (2017).

Supplementary Data, Supplementary Data File 1: includes supplementary figures S1-S6 and a detailed description of the analytical techniques and sample information; Supplementary Data File 2: includes supplementary tables S1-S4.

Figure 1

[Click here to access/download:Figure:Figure 1.eps](#)

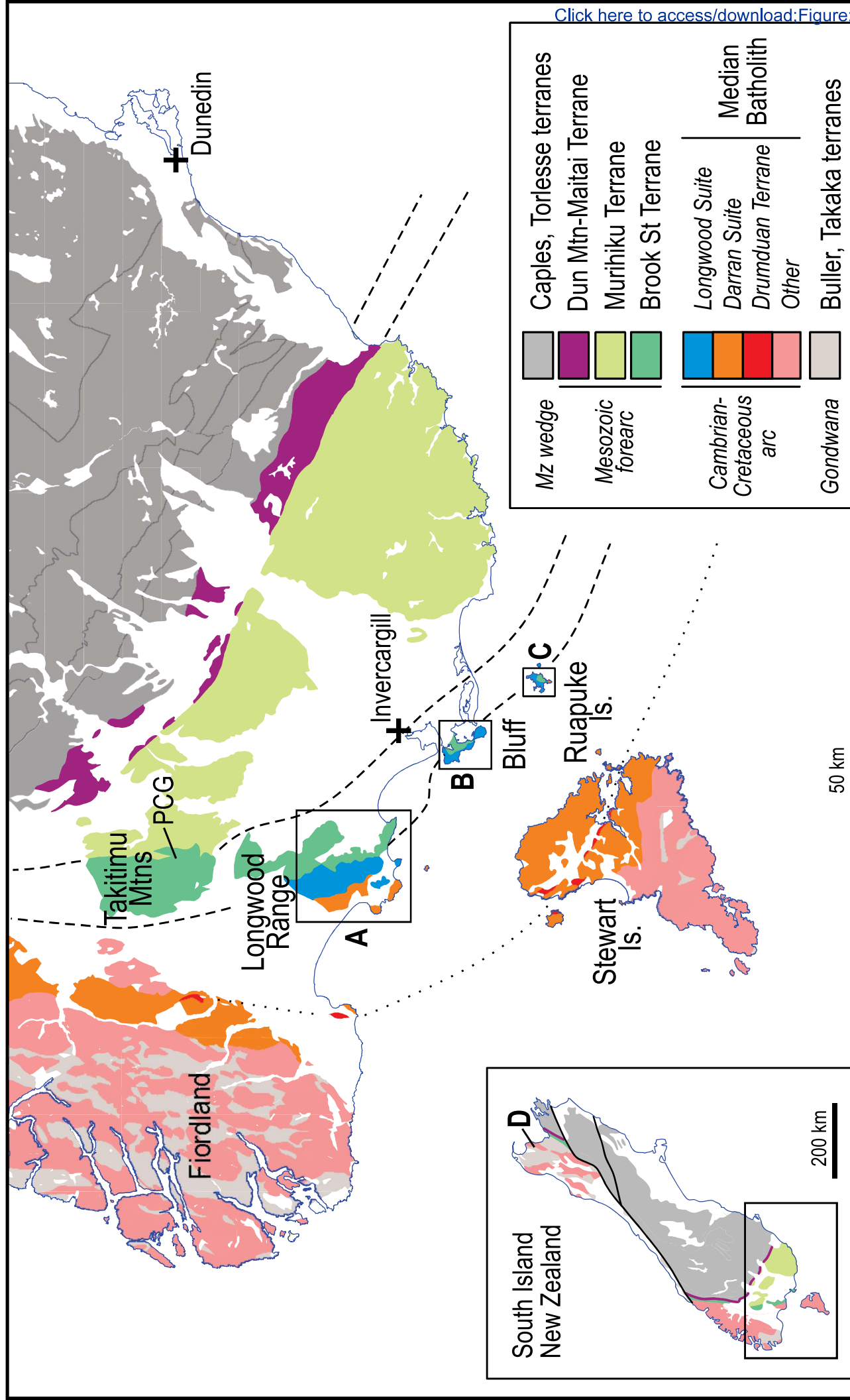


Figure 2

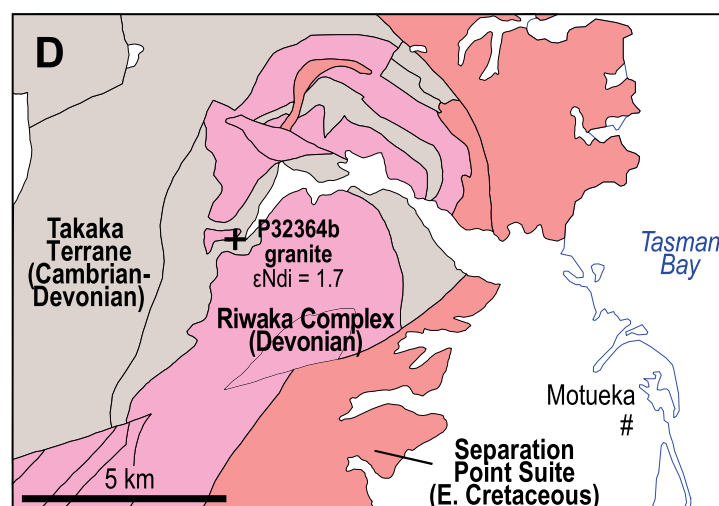
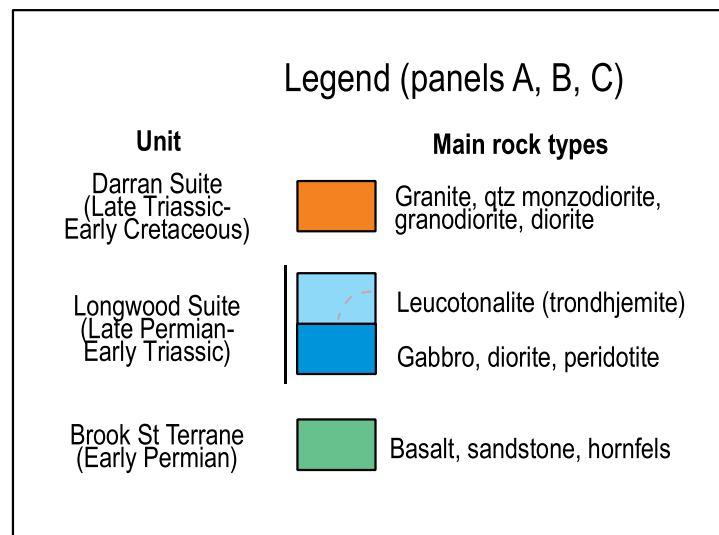
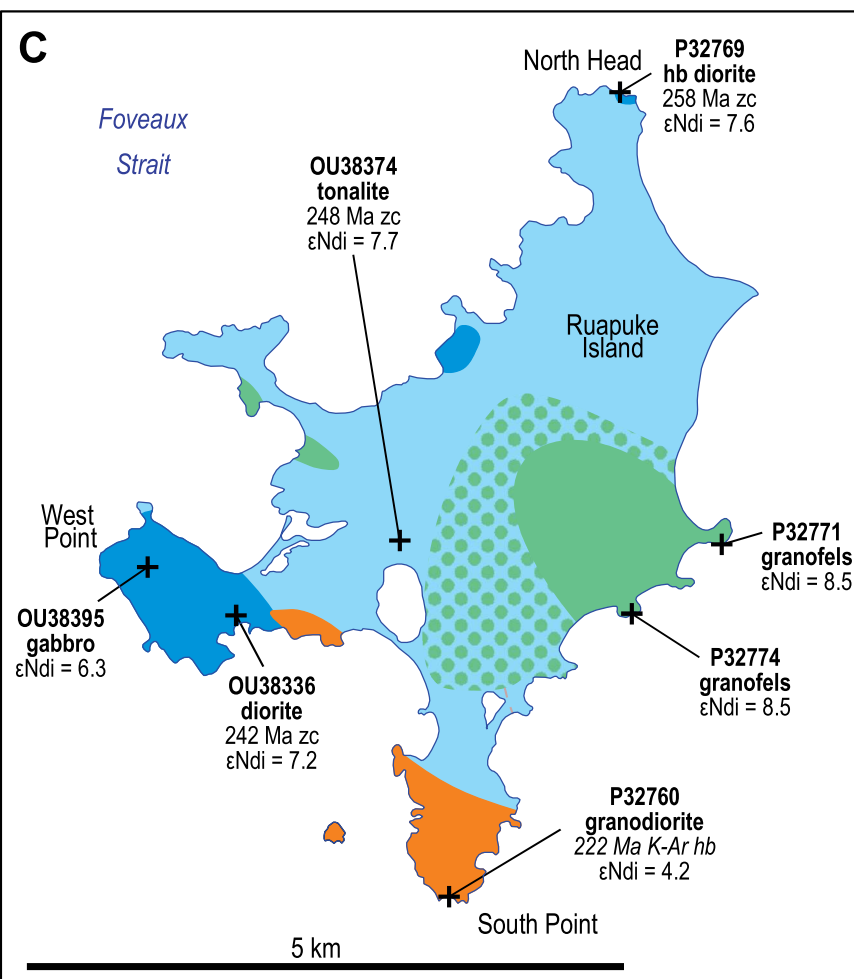
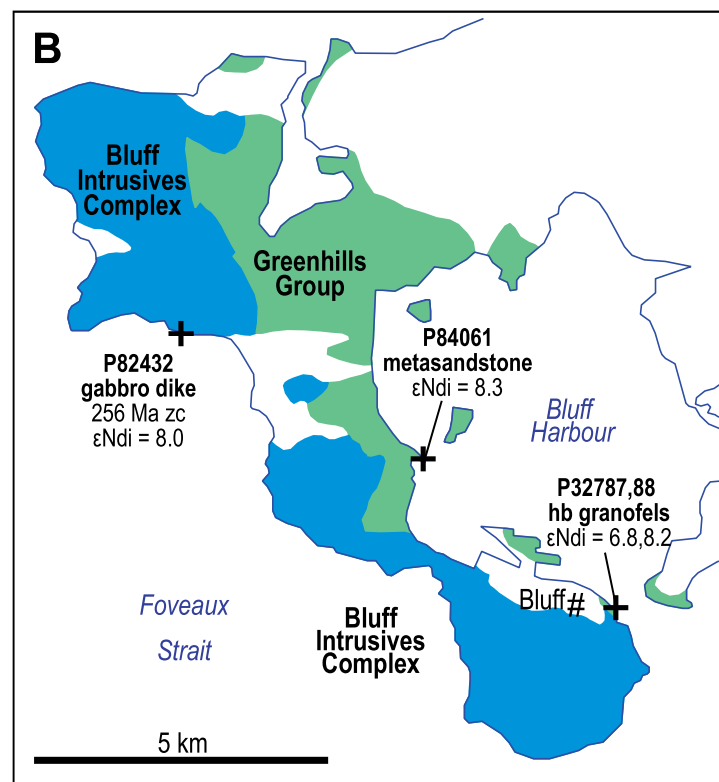
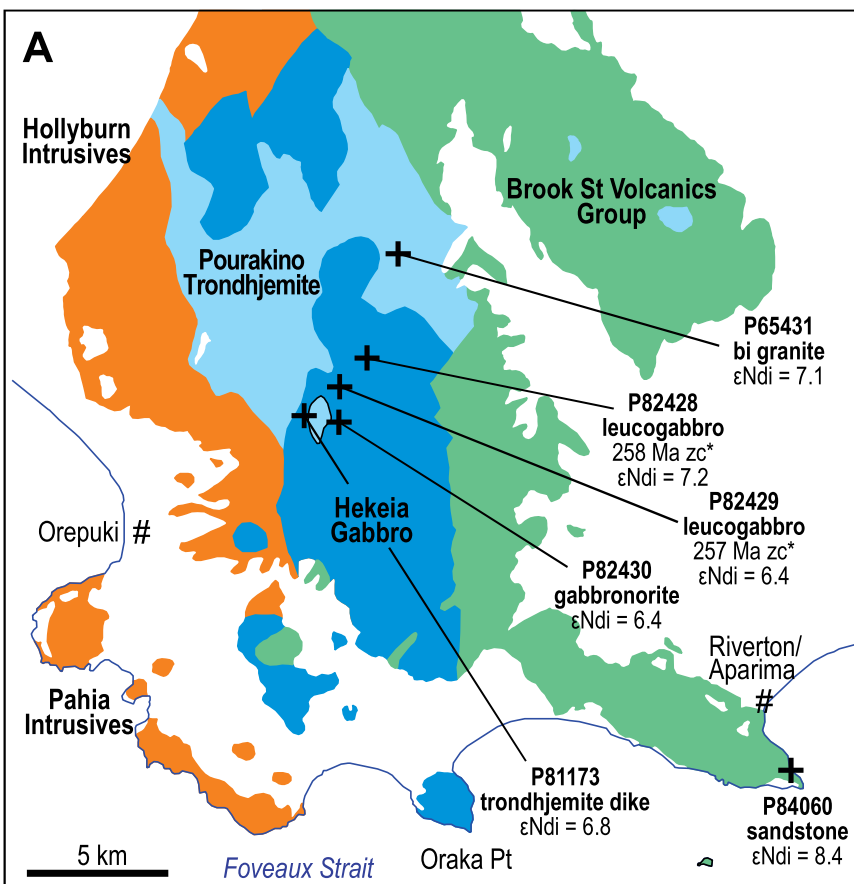
[Click here to access/download;Figure;Figure 2.eps](#)

Figure 3

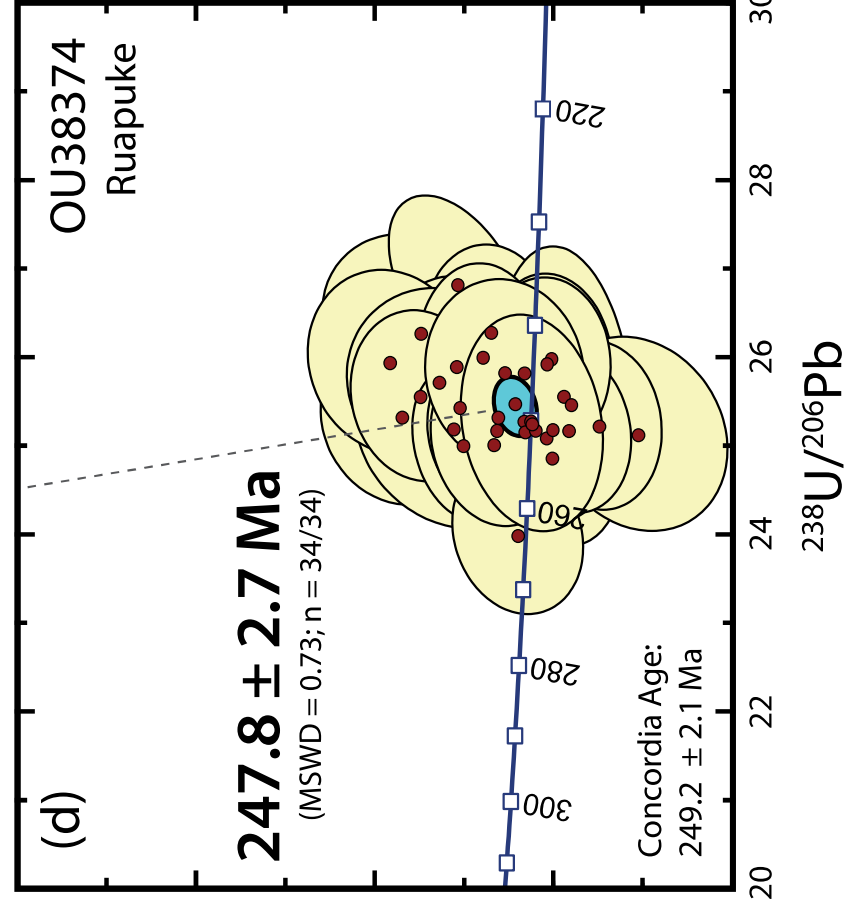
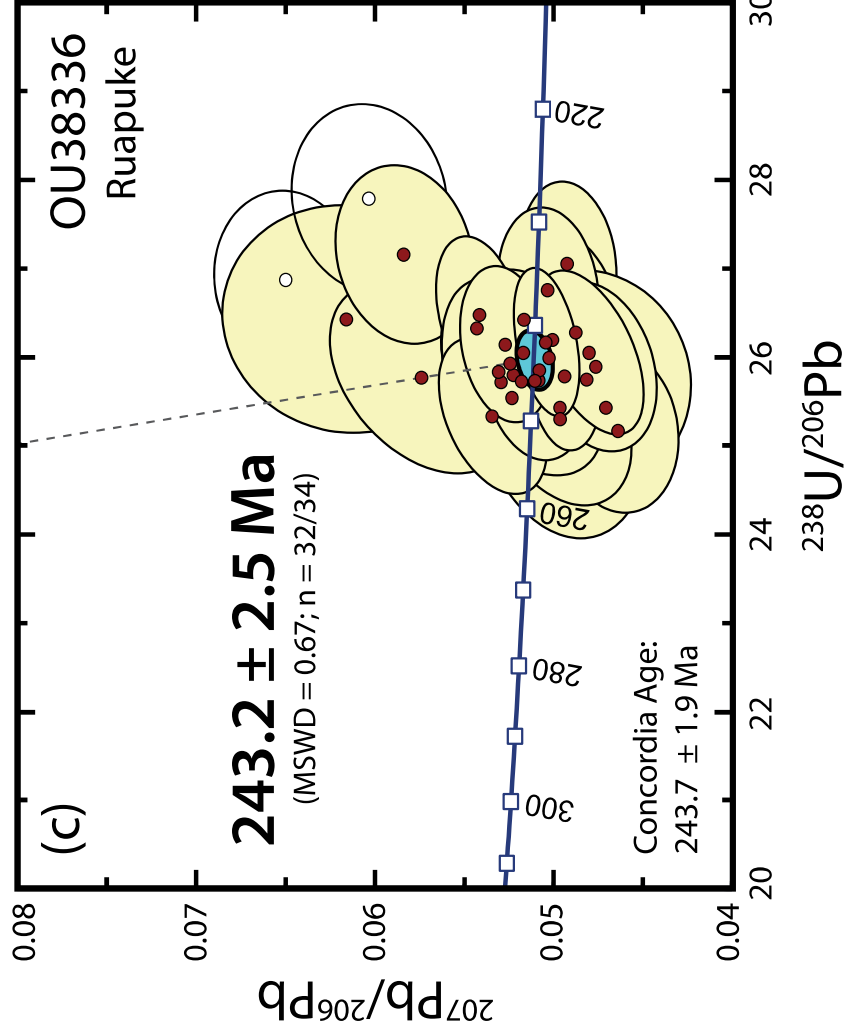
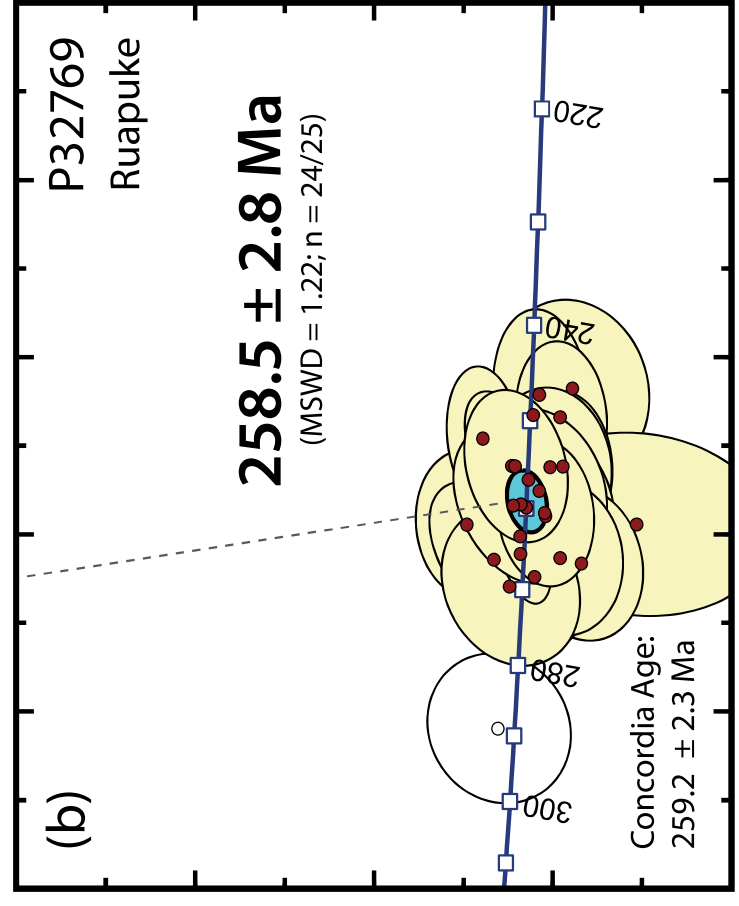
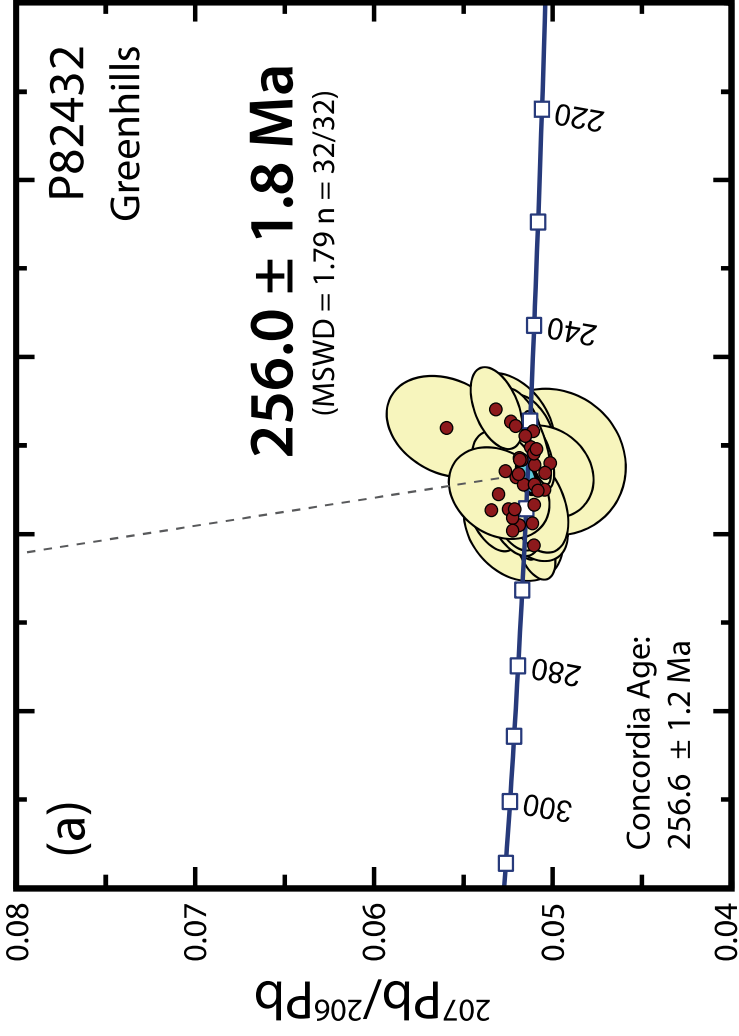


Figure 4

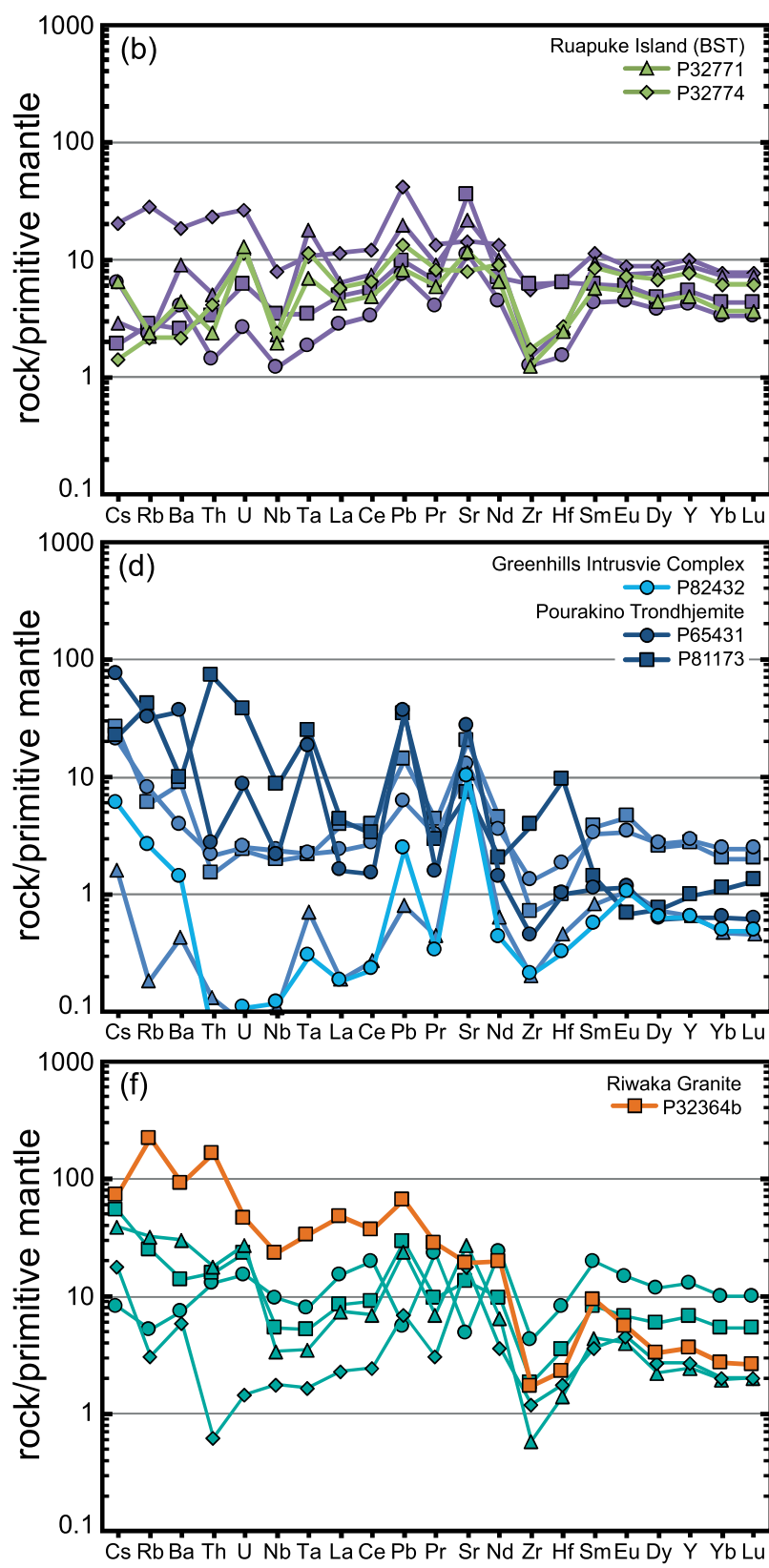
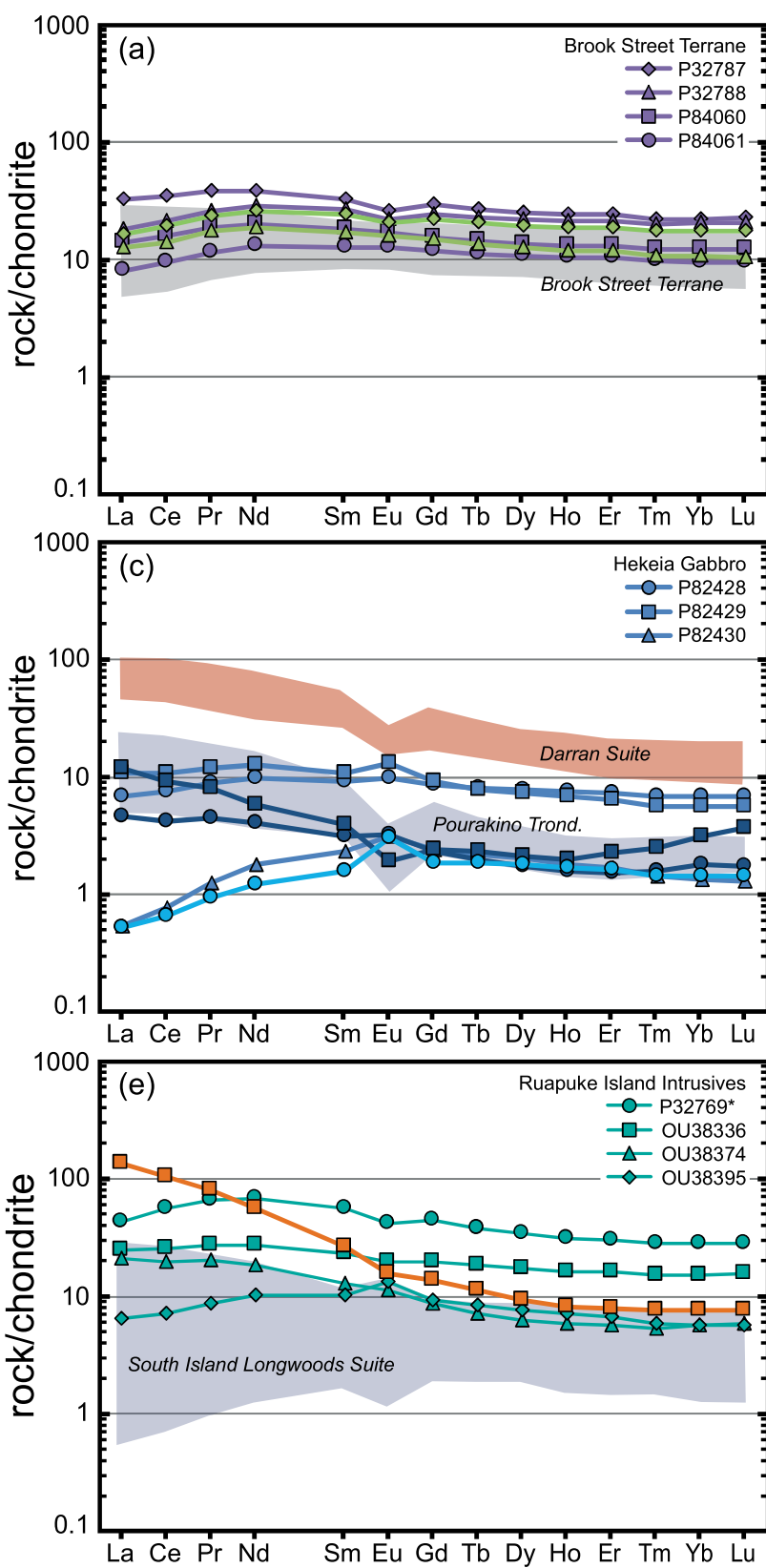
[Click here to access/download;Figure;Figure 4.eps](#)

Figure 5

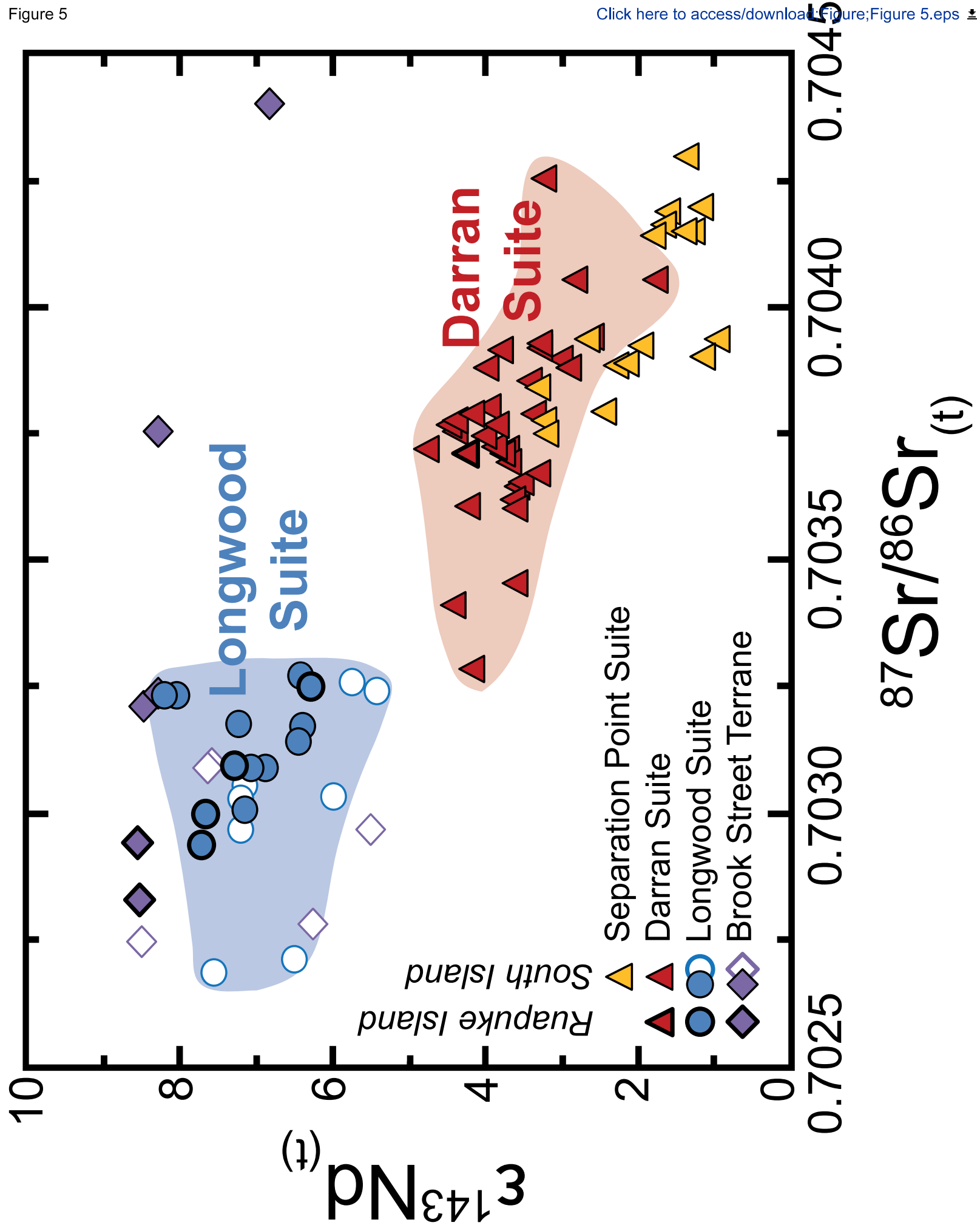
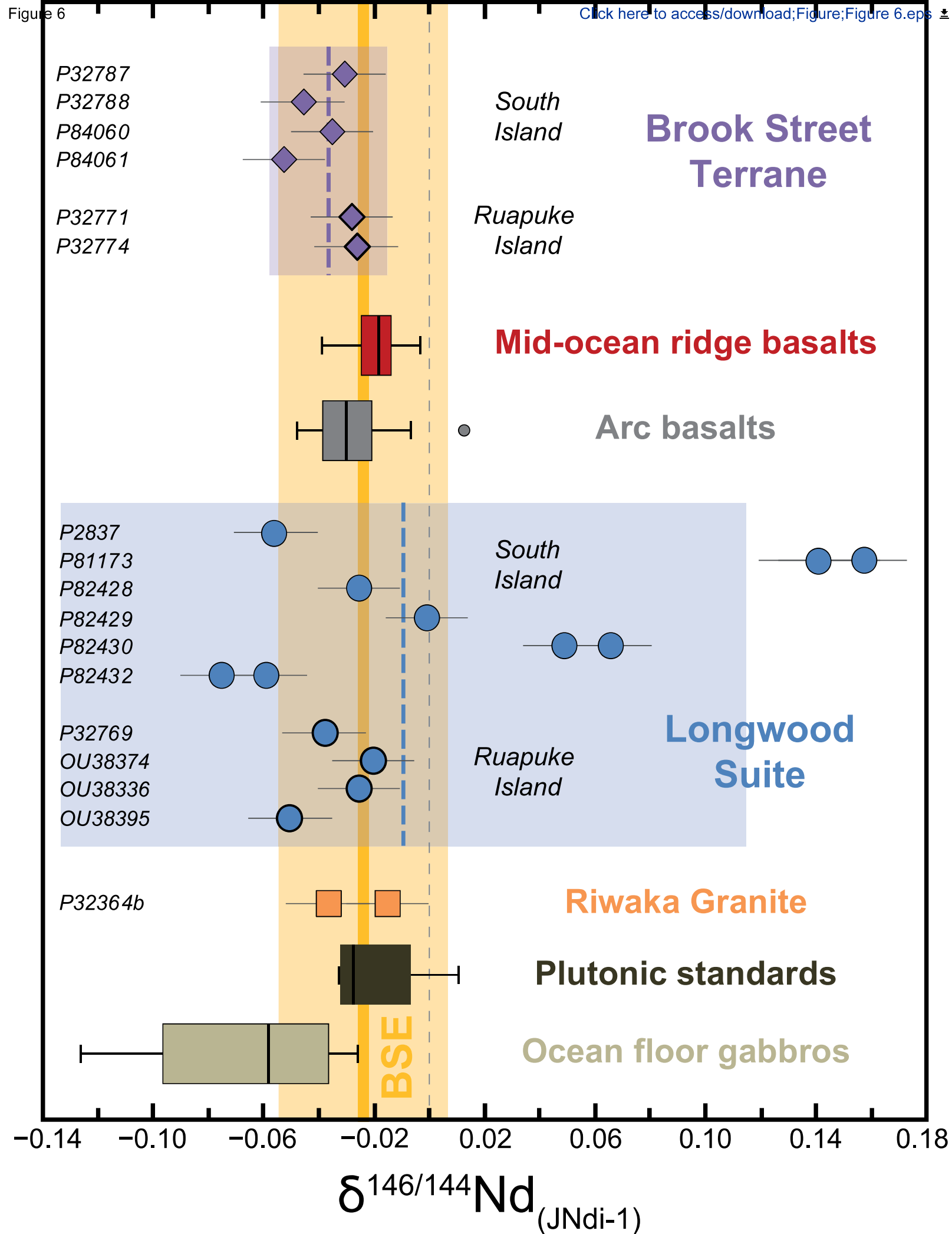
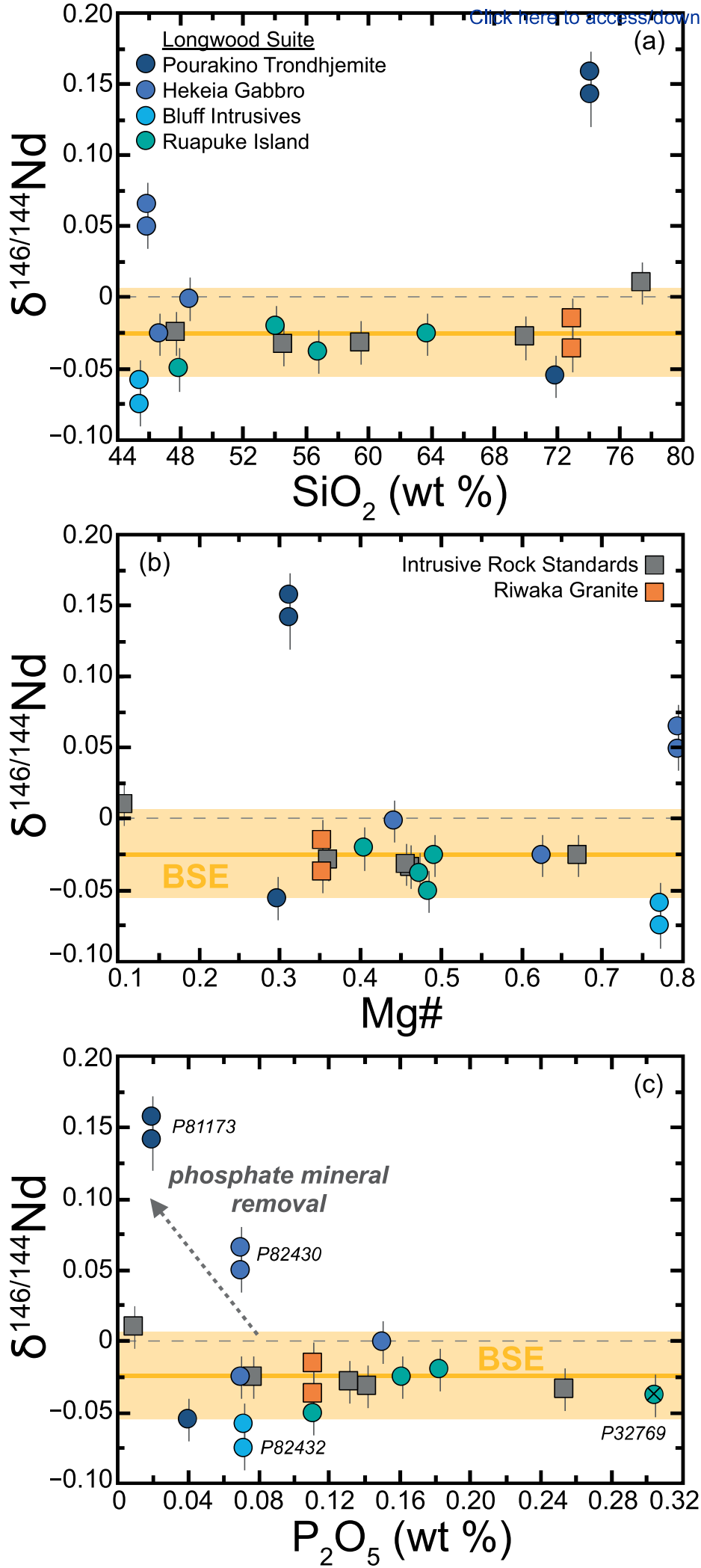


Figure 6





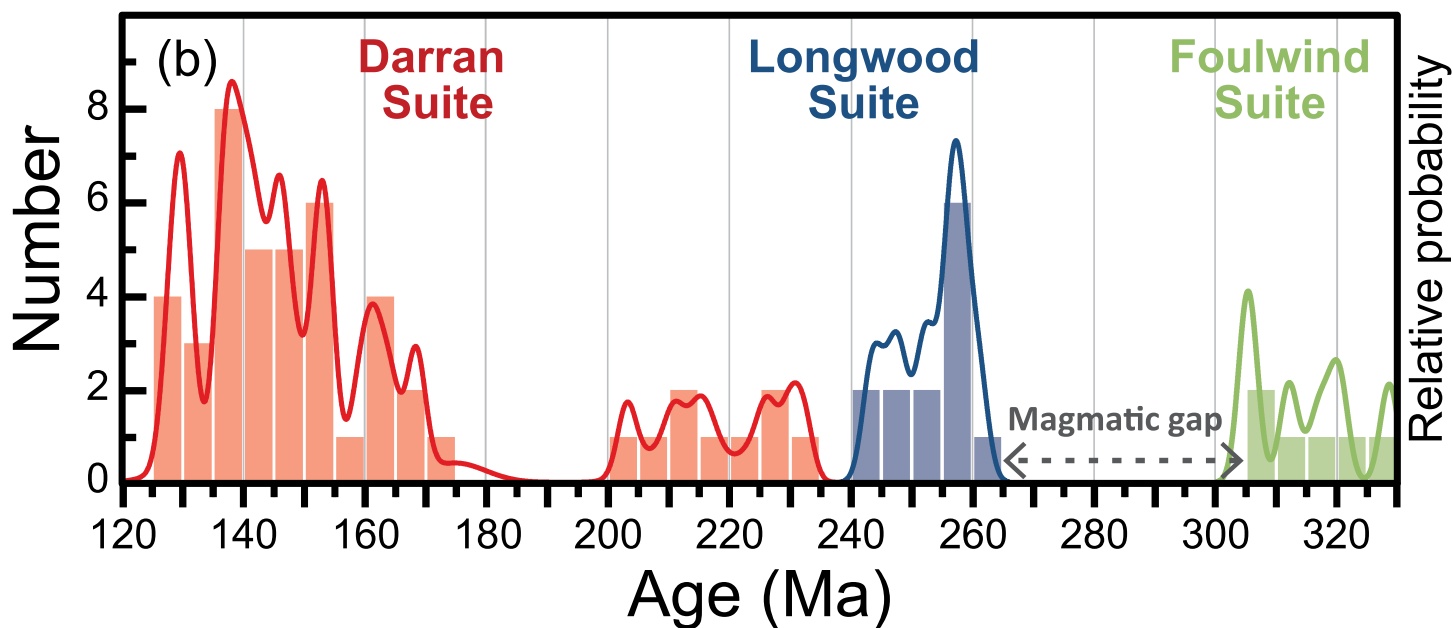
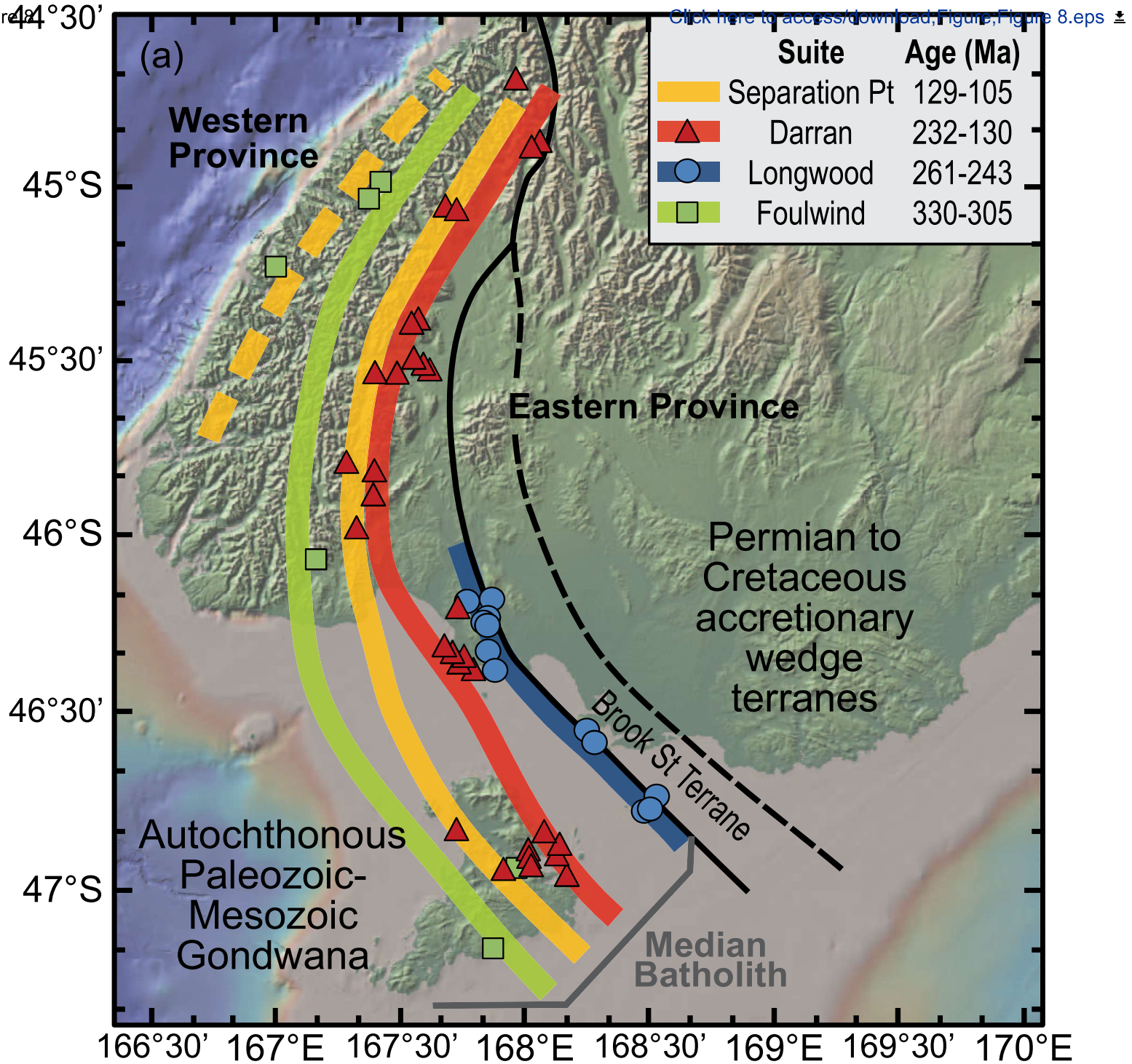
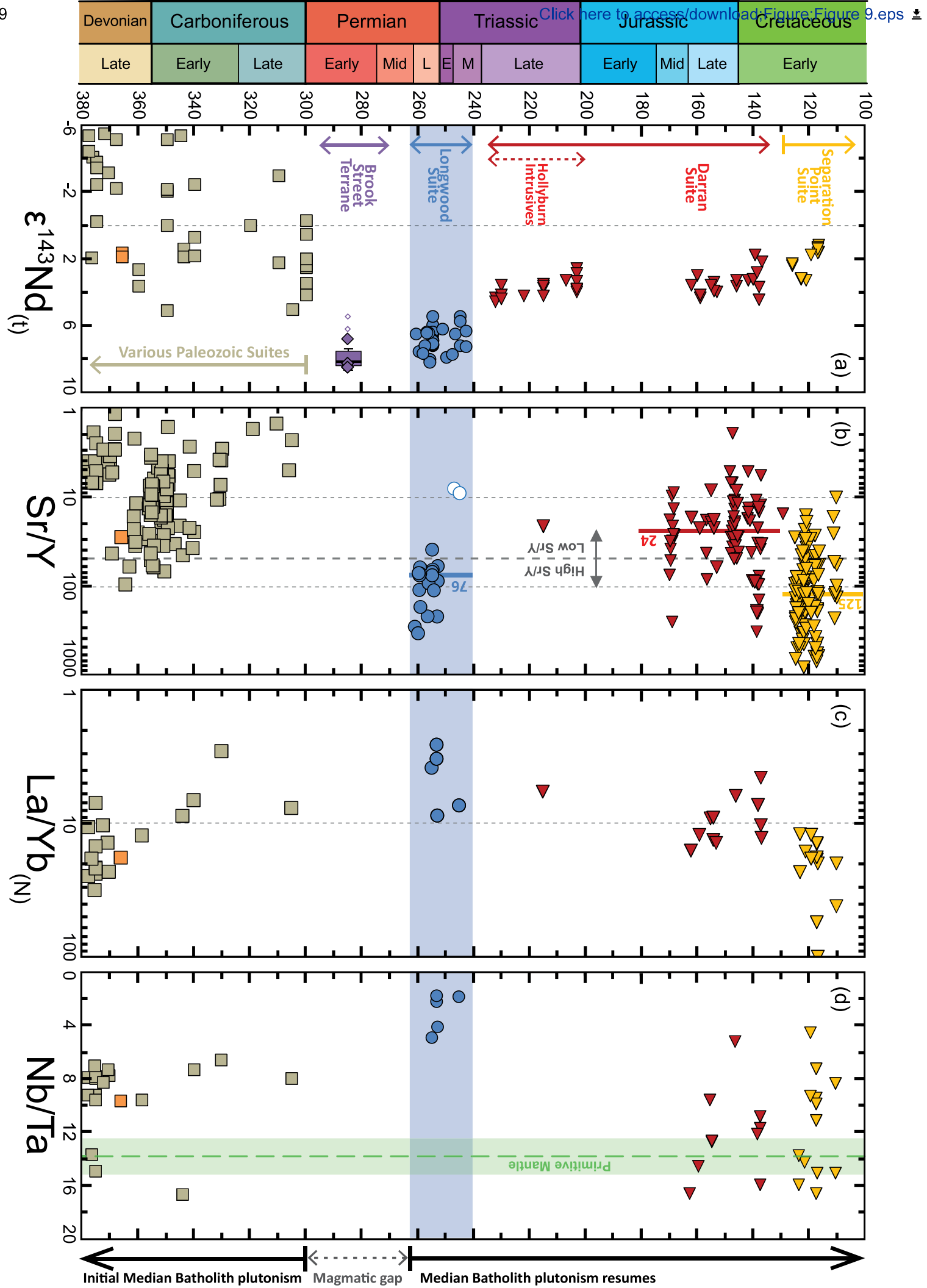


Figure 9



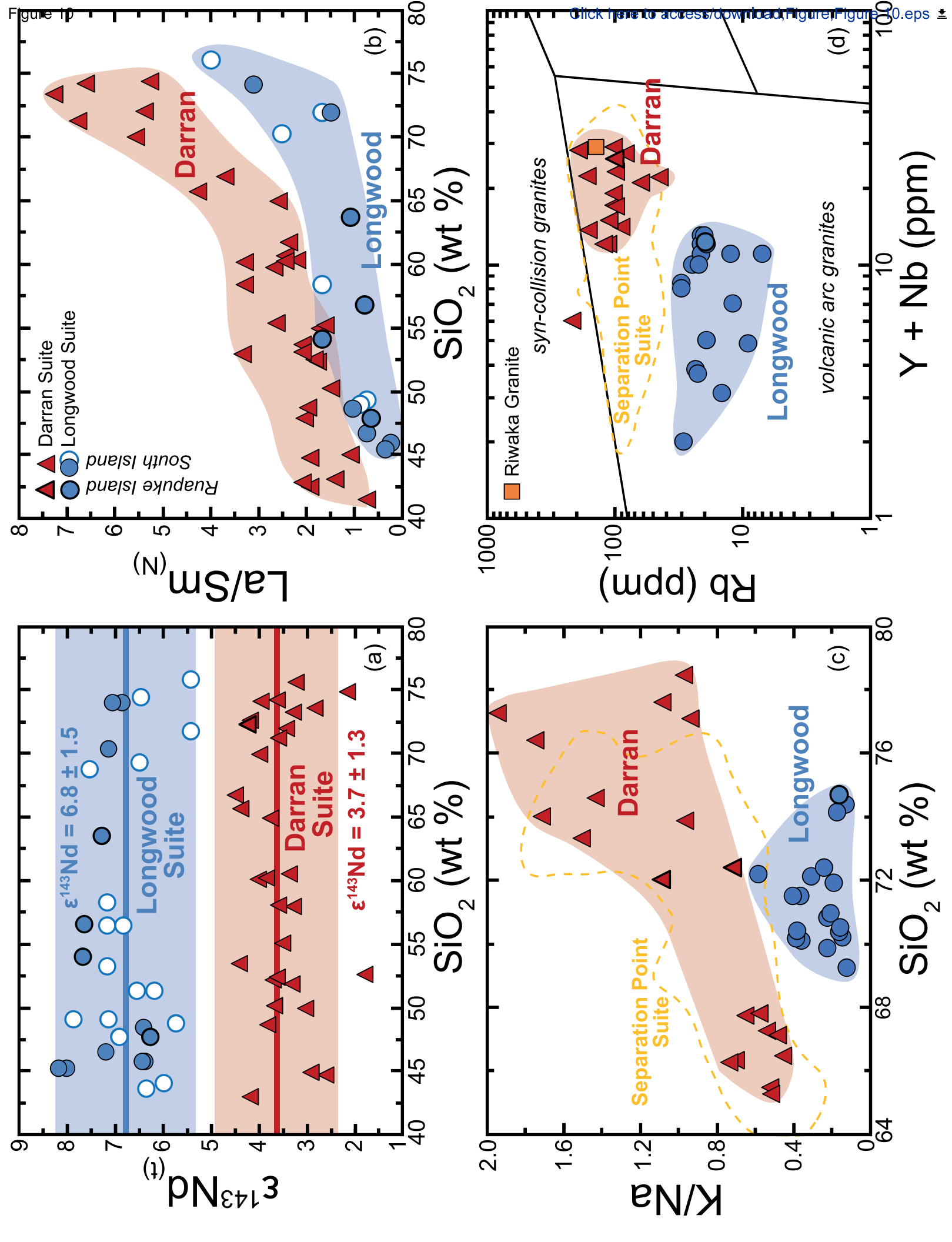


Figure 11

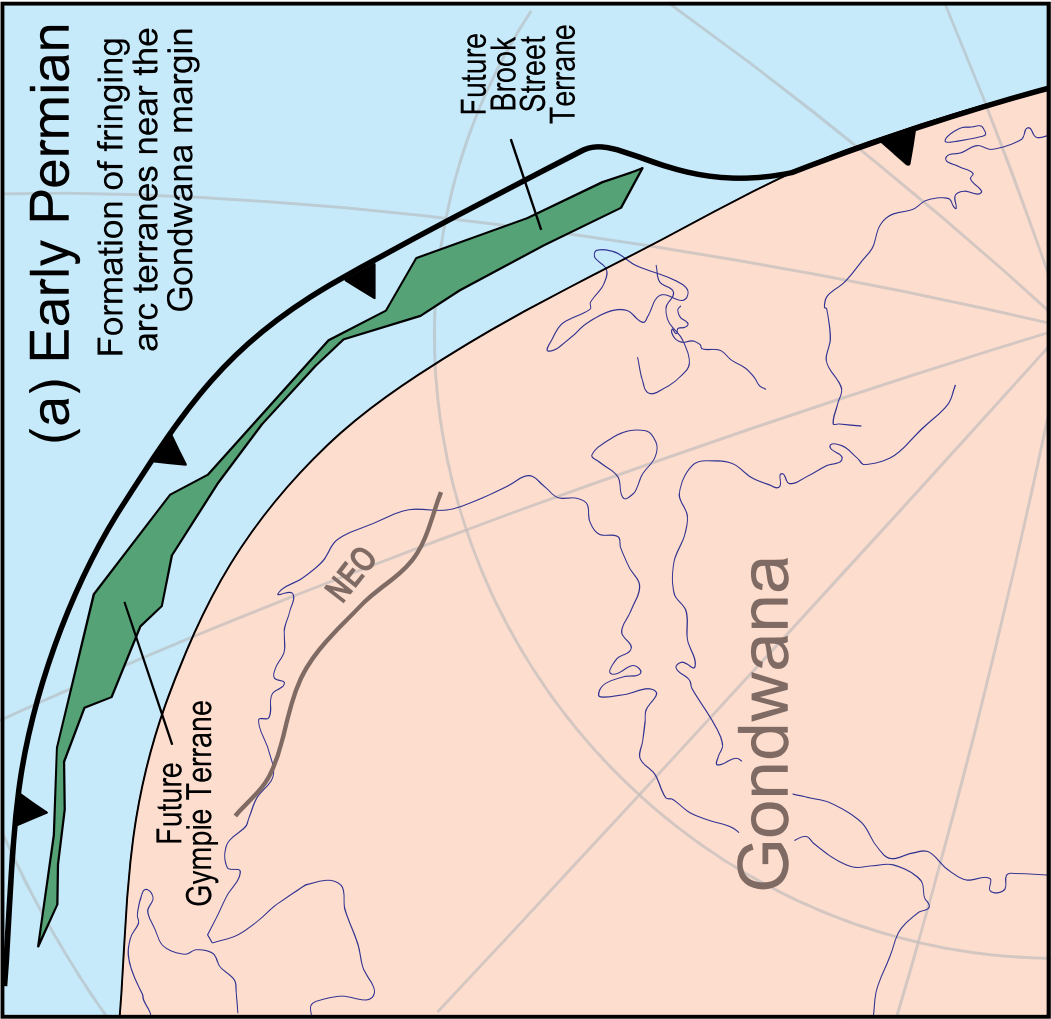
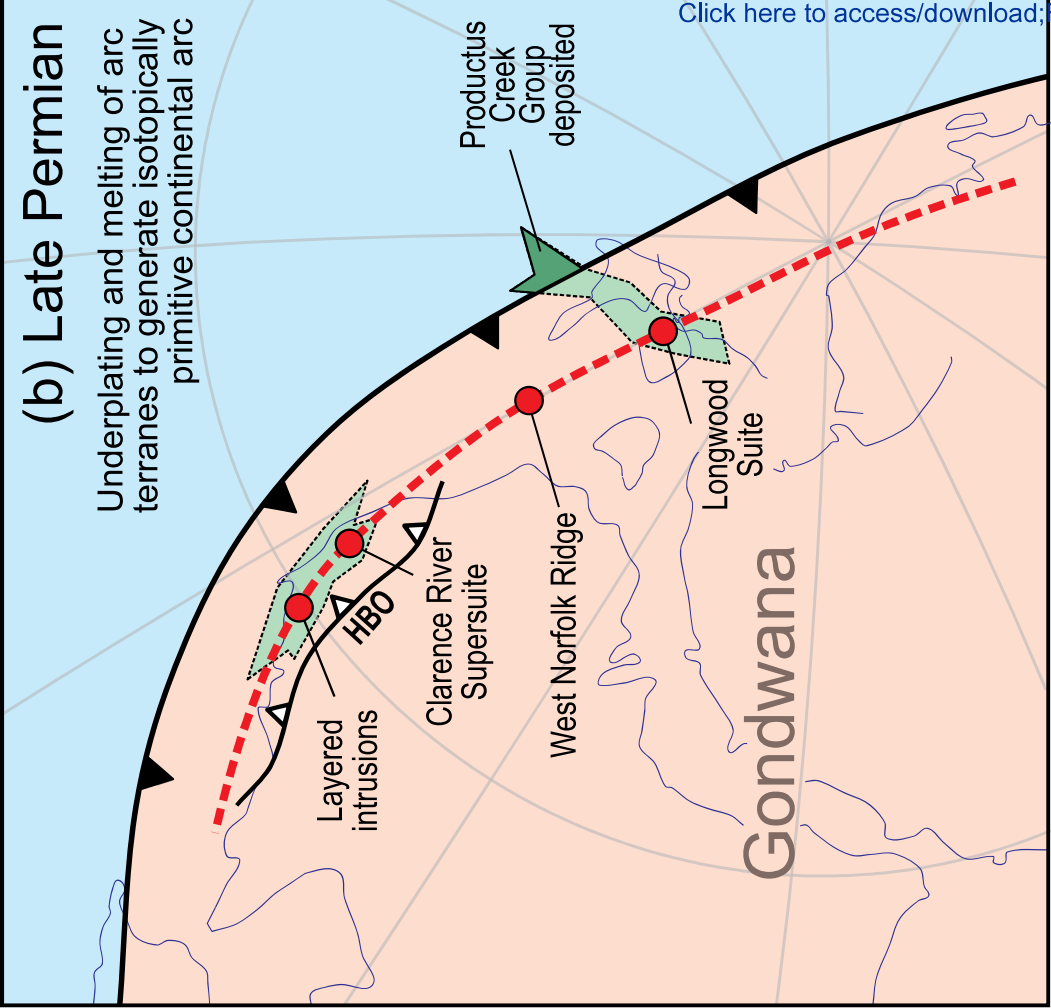


Table 1: Summary of SHRIMP U-Pb zircon data for intrusive rocks of the Longwood Suite.

Sample	Rock type	Location	Unit	²⁰⁶ Pb/ ²³⁸ U Mean Age (Ma)	n	MSWD
P82432	Gabbro dike	Green Hills Intrusion, Bluff Peninsula	Bluff Intrusive Complex	256.0 ± 1.8	32/32	1.79
P32769	Diorite	North Head, Ruapuke Island	Ruapuke Intrusive Complex	258.5 ± 2.8	24/25	1.22
OU38336	Diorite	West Point, Ruapuke Island	Ruapuke Intrusive Complex	243.2 ± 2.4	32/34	0.67
OU38374	Tonalite	Waitokariro Lagoon, Ruapuke Island	Ruapuke Intrusive Complex	247.8 ± 2.7	34/34	0.73

Table 2: Whole rock Rb-Sr, Sm-Nd and Nd stable isotope data

Sample	Unit	Age (Ma)	¹⁴⁷ Sm/ ¹⁴⁴ Nd	¹⁴³ Nd/ ¹⁴⁴ Nd	¹⁴³ Nd/ ¹⁴⁴ Nd _(t)	⁸⁷ Rb/ ⁸⁶ Sr	⁸⁷ Sr/ ⁸⁶ Sr	⁸⁷ Sr/ ⁸⁶ Sr _(t)	Nd (ppm)	δ ^{146/144} Nd	δ ^{148/144} Nd	δ ¹⁴⁶ Nd _(NORM)
Brook Street Terrane												
<i>Southern South Island</i>												
Greenhills												
P32787^	Group	285*	0.1675	0.512933 ±3	0.51263	6.79	0.1583	0.705040 ±7	0.70442	18.77	-0.027 ±0.005	-0.073 ±0.011 ±0.005
Greenhills												
P32788	Group	285*	0.1839	0.513037 ±3	0.51271	8.25	0.0080	0.703269 ±7	0.70324	13.89	-0.042 ±0.005	-0.071 ±0.012 ±0.005
Brook St												
Volcanics												
P84060	Group	285*	0.1731	0.513027 ±3	0.51272	8.43	0.0061	0.703237 ±4	0.70321	9.92	-0.032 ±0.005	-0.061 ±0.012 ±0.005
Greenhills												
P84061^	Group	285*	0.1887	0.513047 ±5	0.51271	8.26	0.0169	0.703821 ±4	0.70375	6.14	-0.049 ±0.008	-0.098 ±0.020 ±0.009
<i>Ruapuke Island</i>												
Greenhills												
P32771	Group	285*	0.1761	0.513035 ±2	0.51272	8.48	0.0163	0.702895 ±4	0.70283	8.91	-0.024 ±0.004	-0.030 ±0.010 ±0.005
Greenhills												
P32774	Group	285*	0.1818	0.513047 ±2	0.51272	8.52	0.0216	0.703031 ±3	0.70295	12.18	-0.023 ±0.004	-0.028 ±0.009 ±0.004
Longwood Suite												
<i>Southern South Island</i>												
Pourakino												
P65431	Trond.	255 ^s	0.1520	0.512928 ±2	0.51267	7.12	0.0935	0.703350 ±4	0.70301	1.87	-0.052 ±0.004	-0.098 ±0.011 ±0.005
Pourakino												
P81173	Trond.	255 ^s	0.1332	0.512883 ±13	0.51266	6.85	0.4604	0.704764 ±3	0.70310	2.77	0.145 ±0.022	0.296 ±0.053 ±0.022
P81173#												
Hekeia												
P82428	Gabbro	257.60	0.1846	0.512986 ±4	0.51267	7.18	0.0509	0.703366 ±4	0.70318	4.87	0.161 ±0.003	0.296 ±0.008 ±0.004
Hekeia												
P82429	Gabbro	256.50	0.1666	0.512915 ±3	0.51264	6.39	0.0230	0.703359 ±5	0.70327	5.81	0.002 ±0.006	-0.006 ±0.014 ±0.006

	Hekeia	0.513067		0.703180	0.069	0.111	0.065
P82430	Gabbro	257 ^s 0.2575	±3	0.51263 6.37 0.0014	±6 0.70317 0.80	±0.012	±0.005
		0.513069		0.703151	0.053	0.097	0.049
P82430#		±3		±4 0.70315 0.73	±0.005	±0.012	±0.005
	Bluff	0.513149		0.703313	-0.055	-0.107	-0.059
P82432	Intrusives	256.0 0.2567	±3	0.51272 8.00 0.0205	±4 0.70324 0.54	±0.015	±0.006
		0.513157			-0.072	-0.185	-0.075
P82432#		±4		0.51273 8.17	±0.006	±0.015	±0.007

Ruapuke Island

	Ruapuke	0.512968		0.703311	-0.035	-0.049	-0.038
P32769	Intrusives	258.5 0.1610	±2	0.51270 7.61 0.0832	±4 0.70300 32.49	±0.010	±0.005
	Ruapuke	0.512932		0.703275	-0.017	-0.031	-0.021
OU38374	Intrusives	247.8 0.1355	±3	0.51271 7.67 0.0938	±4 0.70294 8.95	±0.011	±0.005
	Ruapuke	0.512960		0.703610	-0.022	-0.063	-0.026
OU38336	Intrusives	243.2 0.1659	±2	0.51270 7.25 0.1474	±4 0.70310 13.17	±0.010	±0.005
	Ruapuke	0.512955		0.703301	-0.047	-0.084	-0.051
OU38395	Intrusives	250 ^s 0.1942	±3	0.51264 6.26 0.0140	±4 0.70325 4.96	±0.013	±0.006

Paringa Suite

Northwest Nelson

	Riwaka	0.512467		0.709524 0.70470	-0.033	-0.066	-0.037
P32364b	Granite	364 0.0916	±3	0.51225 1.55 0.9313	±4 27.18	±0.011	±0.005
		0.512481			-0.012	-0.051	-0.015
P32364b#		±3		0.51226 1.81	±0.004	±0.011	±0.005

Table 3: Calculated time-averaged areal magma addition rates for the Longwood, Darran and Separation Point suites.

Suite and region	Age range (Ma)	Duration (Ma)	Area (km²)	Magma addition rate (km²/Ma)
<i>Longwood Suite</i>				
Longwood Range (Hekeia Gabb., Pourakino Tr.)	261-245	16	164	10
Bluff Intrusive Complex, Ruapuke Island	259-243	16	37	2
<i>Total onland exposure</i>	<i>261-243</i>	<i>18</i>	<i>201</i>	<i>11</i>
<i>Total including offshore interpolation</i>	<i>261-243</i>	<i>18</i>	<i>770</i>	<i>43</i>
<i>Darran Suite</i>				
Longwood Range (Hollyburn, Pahia intrusives)	232-202	29	83	3
Eastern Fiordland	167-127	40	2700	67
<i>Total onland exposure</i>	<i>232-130</i>	<i>102</i>	<i>2783</i>	<i>27</i>
<i>Separation Point Suite</i>				
Eastern Fiordland	125-115	10	1050	105
Western Fiordland	125-115	10	2700	270
<i>Total onland exposure</i>	<i>125-115</i>	<i>10</i>	<i>3750</i>	<i>375</i>